A shared regulatory network allows functional coupling of Pho89 and Ena1 in response to environmental alkalinization

Albert Serra Cardona

May 2015

Universitat Autònoma
de Barcelona

A shared regulatory network allows functional coupling of Pho89 and Ena1 in response to environmental alkalinization.

Doctoral thesis presented by

ALBERT SERRA i CARDONA

for the degree of PhD in Biochemistry, Molecular Biology and Biomedicine
from the Universitat Autònoma de Barcelona.

Thesis performed at the Departament de Bioquímica i Biologia Molecular of the Universitat Autònoma de Barcelona and at the Institut de Biotecnologia i de Biomedicina.

Thesis supervised by **Dr. Joaquín Ariño Carmona**

Albert Serra i Cardona

Dr. Joaquín Ariño Carmona

Cerdanyola del Vallès, May 2015

TABLE OF CONTENTS

I. ABBREVIATIONS 1

II. SUMMARIES 7

III. INTRODUCTION 11

1. The model organism *Saccharomyces cerevisiae* 13

2. Alkaline pH adaptation of *S. cerevisiae* 14

2.1. The Rim101 pathway 16

2.2. The calcineurin pathway 19

2.3. The Snf1 pathway 24

2.4. Other pathways involved in alkaline pH adaptation 33

2.5. The *ENA1* Na^+-ATPase 37

2.6. Alkaline pH adaptation in other fungi 39

3. Phosphate homeostasis 44

3.1. Phosphate homeostasis under non-limiting conditions 44

3.2. Phosphate homeostasis under limiting conditions: the *PHO* regulon 46

3.3. The *PHO* signaling pathway 48

4. Pho89 54

4.1. Sodium-phosphate cotransport in *S. cerevisiae* 54

4.2. The regulation of *PHO89* 56

IV. OBJECTIVES 57

V. EXPERIMENTAL PROCEDURES 61

1. Yeast strains and media 63

2. Recombinant DNA techniques 63

3. Deletion cassettes and gene disruptions 64

4. Plasmids 66

5. Growth assays 67

6. β-galactosidase assays 67

7. RT-PCR and qRT-PCR 68

8. Chromatin immunoprecipitation 69

9. Protein immunodetection 71

  9.1. Sample collection 71

  9.2. Extracts preparation 72

  9.3. SDS-PAGE and immunobloting 73

10. Determination of intracellular sodium accumulation 74

11. Microscopy 74

VI. RESULTS AND DISCUSSION 77

1. Analysis of the promoter region of *PHO89* 79

2. Expression profiles of Pho89 and Pho84: a comparative analysis 81

  2.1. Pho89 is rapidly induced by high pH stress and upregulated by Pho4 81

  2.2. Pho84 and Pho89 display remarkable differences in their expression under low P_i or alkaline conditions 83

3. The role of the calcineurin pathway in *PHO89* alkaline induction 86

  3.1. The alkaline induction of Pho89 is strongly dependent on calcineurin 86

  3.2. The calcineurin pathway upregulates *PHO89* through Crz1 binding to its promoter 87

4. The effect of the Rim101 and Snf1 pathways on *PHO89* alkaline induction 90

  4.1. Rim101 and Snf1 are required to induce the expression of *PHO89* under alkaline conditions 90

  4.2. The absence of Rim101 or Snf1 results in different Pho89 expression kinetics 92

5. The role of the Rim101 pathway in *PHO89* alkaline induction 94

6. The role of the Snf1 pathway in *PHO89* alkaline induction 96

  6.1. Impact of the Snf1 pathway on *PHO89* through Nrg1 and Nrg2 96

6.2. Snf1 upregulates *PHO89* through Mig2 97

6.3. Mig1 and Mig2 are transiently phosphorylated by alkaline stress in a Snf1-dependent manner 99

6.4. Mig1 and Mig2 exit the nucleus during high pH stress 101

6.5. Snf1 is rapidly but transiently phosphorylated after alkaline pH stress 104

6.6. The absence of Reg1 causes a drastic upregulation of Pho89 105

7. Coordinated expression of Pho89 and Ena1 allows functional coupling of both transporters 112

7.1. The *PHO89* promoter is not salt responsive 112

7.2. Pho89 and Ena1 show similar expression profiles under alkaline stress 114

7.3. The absence of Ena1 strongly impairs growth under alkaline conditions of a *pho84* mutant strain 115

7.4. Unrestricted Pho89 activity could lead to toxic sodium accumulation 117

7.5. Gene coregulation analysis as a tool to study protein function 120

VII. CONCLUSIONS 123

VIII. REFERENCES 127

IX. ANNEXES 153

ABBREVIATIONS

ADP	**A**denosine **d**i**p**hosphate
AICAR	5'-phosphoribosyl-5-**a**mino-4-**i**midazole **car**boxamide
AMP	**A**denosine **m**ono**p**hosphate
AMPK	**AMP**-activated protein **k**inase
ATP	**A**denosine **t**ri**p**hosphate
bHLH	Basic **h**elix-loop-**h**elix
bp	Base **p**air
cAMP	Cyclic **AMP**
CDK	Cyclin-**d**ependent **k**inase
CDRE	Calcineurin-**d**ependent **r**esponse **e**lement
ChIP	C**h**romatin immuno**p**recipitation
CoA	C**o**enzyme **A**
C-terminal	Carboxyl t**erminal**
CWI	Cell **w**all **i**ntegrity
DAPI	4',6-**dia**midino-2-**p**henyl**i**ndole
DNA	Deoxyribonucleic acid
EDTA	Ethylene**d**iamine**t**etraacetic **a**cid
ESCRT	Endosomal **s**orting **c**omplex **r**equired for **t**ransport
g	Grams
GABA	**γ**-Amino**b**utyric **a**cid
GFP	Green fluorescent **p**rotein
GTP	Guanosine **t**ri**p**hosphate
H	Hours
HA	Hem**a**gglutinin
IgG	Immuno**g**lobulin **G**
IP$_4$	**I**nositol tetrakis**p**hosphate
IP$_5$	**I**nositol pentakis**p**hosphate
IP$_6$	**I**nositol hexakis**p**hosphate
IP$_7$	Inositol heptakis**p**hosphate
kDa	Kilo **da**ltons
kbp	Kilo **b**ase **p**airs

Abbreviations

Km	Michaelis constant
LB	Lysogeny broth
MAP	Mitogen-activated protein
MAPK	Mitogen-activated protein kinase
MAPKK	Mitogen-activated protein kinase kinase
MAPKKK	Mitogen-activated protein kinase kinase kinase
Mbp	Mega base pairs
µg	microgram
µM	micromolar concentration
mg	milligram
Min	Minute
mm	millimeter
M	Molar concentration
mM	millimolar concentration
mRNA	Messenger RNA
NFAT	Nuclear factor of activated T-cells
ng	nanogram
nm	nanometer
Nt	Nucleotide
N-terminal	Amino terminal
OD	Optical density
ONPG	o-nitrophenyl-β-D-galactopyranoside
PCR	Polymerase chain reaction
P_i	Inorganic phosphate
PKA	Protein kinase A
PMSF	Phenylmethanesulfonylfluoride
PolyP	Polyphosphate
qRT-PCR	quantitative RT-PCR
RNA	Ribonucleic acid
ROS	Reactive oxygen species
rRNA	Ribosomal RNA

RT-PCR	Reverse transcription-PCR
SDS	Sodium dodecyl sulfate
SDS-PAGE	SDS-Polyacrylamide gel electrophoresis
Sec	Second
STRE	Stress response element
TAPS	3-[[1,3-dihydroxy-2-(hydroxymethyl)propan-2-yl]amino]propane-1-sulfonic acid
TBS	Tris-buffered saline
Tris	2-Amino-2-hydroxymethyl-propane-1,3-diol
tRNA	Transfer RNA
UTR	Untranslated region
V-ATPase	Vacuolar-ATPase
VTC	Vacuolar transmembrane chaperone
YNB	Yeast nitrogen base
YPD	Yeast extract peptone dextrose

SUMMARIES

Microorganisms are exposed to slight changes in the environment, which may imply a stressful situation. The budding yeast *Saccharomyces cerevisiae* prefers acidic conditions to proliferate; hence, an alkalinization of the external medium impairs its growth. To cope with this stress, *S. cerevisiae* activates several signaling pathways that create a complex regulatory network, leading to a profound remodeling of the transcriptional profile. The calcineurin pathway, activated by an increase of cytosolic calcium occurring in alkaline conditions, governs gene expression through the transcription factor Crz1. Moreover, high pH stress is sensed by the transmembrane protein Rim21, a component of the Rim101 pathway, which starts a signaling cascade resulting in the proteolytic activation of Rim101. This transcription factor represses the expression of *NRG1*, another transcriptional repressor, thus indirectly inducing the expression of certain genes. The Snf1 kinase is also activated by alkaline stress and has several targets through which it controls different processes. Among them, Snf1 inhibits the repressors Mig1/Mig2 and Nrg1/Nrg2, alleviating the repression of a diverse group of genes. Furthermore, an increase of the external pH also triggers the *PHO* signaling pathway, related to phosphate scarcity, causing the inactivation of the Pho80-Pho85 complex and the subsequent accumulation of Pho4 into the nucleus. This transcription factor, along with Pho2, is responsible for the expression of the *PHO* regulon, the function of which is to maintain the intracellular phosphate pool. The Na^+-ATPase-encoding gene *ENA1* is an excellent example of coregulation by different signaling pathways. The alkaline induction of this gene depends on Crz1 and on release from the repression by Nrg1, Mig1, and Mig2, triggered by activation of Rim101 and Snf1. Pho89 is a high-affinity sodium/phosphate cotransporter belonging to the *PHO* regulon. Apart from being upregulated by Pho4, under alkaline conditions *PHO89* expression is also dependent on Crz1, being the only *PHO* gene to display such regulation.

In this work we focus on the regulatory network driving the alkaline induction of *PHO89* and its possible role in the high pH stress response. We show that the transcriptional profiles of *PHO89* between alkaline and phosphate starvation conditions differ considerably, with a much weaker and delayed expression on the latter. In contrast, the expression of Pho84, the other high-affinity phosphate transporter, is stronger in low phosphate conditions than under alkaline stress. The calcineurin effect on *PHO89* is mediated exclusively through Crz1, and this transcription factor is bound to its promoter shortly after the alkaline induction. The Rim101 pathway also upregulates *PHO89* during high pH stress by impinging on *NRG1*. After the alkaline stress, the Snf1 kinase is phosphorylated and mediates the phosphorylation of the repressors Mig1 and Mig2, which exit the nucleus under these same conditions. However, only Mig2 has a relevant role in repressing *PHO89*. Furthermore, the *reg1* mutation, which leads to a hyperactive Snf1, results in increased Pho89 levels over time, indicating the importance of Snf1 in the alkaline expression of this transporter.

In this study we also show the putative relationship between Pho89 and Ena1 in an alkaline environment. Both genes share several regulatory factors which allow their synchronous expression after high pH stress. Interestingly, when cells rely exclusively on Pho89 for phosphate uptake, the absence of *ENA1* confers a strong alkali-sensitive phenotype. In this same situation, cells display a substantial increase in their intracellular sodium concentration, suggesting that this might be the cause of impaired growth. These results point towards the idea that the coregulation exhibited by Ena1 and Pho89 could allow their functional coupling, and that the Na^+ extrusion ability of Ena1 could serve as a detoxifying mechanism necessary to support continuous Pho89 Na^+/P_i cotransport under alkaline conditions.

Els microorganismes estan exposats a canvis en l'ambient que poden implicar una situació d'estrès. El llevat *Saccharomyces cerevisiae* prefereix condicions acides per proliferar; per tant, l'alcalinització del medi extern li empitjora el creixement. Per superar aquest estrès, el llevat activa diverses vies de senyalització que conformen una complexa xarxa reguladora, provocant un remodelament transcripcional. La via de la calcineurina, activada per l'increment de calci citosòlic en condicions alcalines, governa l'expressió gènica a través del factor de transcripció Crz1. Un estrès alcalí és detectat per la proteïna transmembrana Rim21, un component de la via Rim101, que desencadena una cascada de senyalització provocant l'activació per proteòlisi de Rim101. Aquest factor de transcripció reprimeix l'expressió de *NRG1*, un altre repressor transcripcional, induint així l'expressió de determinats gens indirectament. La quinasa Snf1 també s'activa per estrès alcalí i té varies dianes a través de les quals controla diferents processos. Entre aquestes, Snf1 inhibeix els repressors Mig1/Mig2 i Nrg1/Nrg2, alleugerint la repressió d'un grup divers de gens. Addicionalment, un increment del pH extern activa la via de senyalització *PHO*, relacionada amb l'escassetat de fosfat, provocant la inactivació del complex Pho80-Pho85 i la subseqüent acumulació de Pho4 al nucli. Aquest factor de transcripció, conjuntament amb Pho2, és responsable de l'expressió del reguló *PHO*, la funció del qual és mantenir els nivells de fosfat intracel·lular. El gen *ENA1*, que codifica una Na^+-ATPasa, és un clar exemple de coregulació per diferents vies de senyalització. La seva inducció alcalina depèn de Crz1 i de l'alliberament de la repressió de Nrg1, Mig i Mig2, els quals son inhibits per Rim101 i Snf1. Pho89 és un cotransportador de sodi/fosfat d'alta afinitat membre del reguló *PHO*. Apart de ser induït per Pho4, sota condicions alcalines l'expressió de *PHO89* també depèn de Crz1, sent l'únic gen del reguló *PHO* que mostra aquesta regulació.

En aquest treball ens centrem en la xarxa reguladora que controla la inducció alcalina de *PHO89* i el seu possible paper en la resposta a aquest estrès. Mostrem com l'expressió de *PHO89* en condicions d'escassetat de fosfat és més feble i retardada en comparació amb l'expressió a pH bàsic. Per altra banda, l'expressió de Pho84, l'altre transportador de fosfat d'alta afinitat, és més potent en condicions de baix fosfat que en condicions d'estrès alcalí. L'efecte de la via de la calcineurina sobre *PHO89* es produeix exclusivament a través de Crz1, i aquest factor de transcripció s'uneix al seu promotor poc després de l'estrès alcalí. La via Rim101 també indueix *PHO89* en condicions de pH bàsic a través de *NRG1*. En condicions alcalines, la quinasa Snf1 és fosforilada i és responsable de la fosforilació dels repressors Mig1 i Mig2, que surten del nucli. Tot i això, només Mig2 té un paper rellevant en la repressió de *PHO89*. A més a més, la mutació *reg1*, que presenta una Snf1 hiperactiva, provoca un increment dels nivells de *PHO89* al llarg del temps.

En aquest treball també mostrem la possible relació entre Pho89 i Ena1 en un ambient alcalí. Tots dos gens comparteixen els mateixos factors reguladors que permeten la seva expressió sincrònica després d'un estrès per pH bàsic. Quan l'adquisició de fosfat depèn exclusivament de Pho89, l'absència de *ENA1* confereix un fort fenotip de sensibilitat a pH alcalí. En aquesta mateixa situació, les cèl·lules presenten un increment substancial en la concentració de sodi intracel·lular, suggerint que aquesta pot ser la causa dels seus problemes de creixement. Aquests resultats indiquen que la coregulació entre Ena1 i Pho89 permetria el seu acoblament funcional, ja que la capacitat per expulsar sodi de Ena1 serviria de mecanisme de detoxificació, permetent un continu cotransport Na^+/P_i en condicions alcalines.

INTRODUCTION

1. The model organism *Saccharomyces cerevisiae*

The budding yeast *Saccharomyces cerevisiae* is a unicellular fungus belonging to the phylum of Ascomycota and to the family of *Saccharomycetaceae*. In nature, it is often found on the skin of ripe fruits such as grapes and has an optimum temperature for growth around 30°C. *S. cerevisiae* laboratory strains exist in two stable forms: haploid and diploid. Haploid cells proliferate through mitosis and are sexually differentiated as mating type **a** or *α*. Two opposite mating types can mate to generate a diploid cell, which can proliferate via mitosis or, under nutrient starvation, undergo meiosis producing four haploid spores. The budding yeast can grow aerobically and anaerobically utilizing several different sugars as carbon source, although glucose is the preferred one. Its genome is composed of 16 chromosomes accounting for 12.1 Mbp and 6000 genes approximately, of which 85% have an annotated biological role.

S. cerevisiae is responsible for the alcoholic fermentation associated with the production of bread or alcoholic beverages like beer or wine. Apart from its obvious importance in the food industry, it is used for the production of various compounds with commercial interest and for heterologous protein expression. Because it is an easy organism to cultivate and manipulate and it does not cause any human infection, it began to be used as a model for genetic and metabolic studies. Since the sequencing of its genome in 1996, being the first eukaryotic organism to be sequenced, it has become an invaluable tool for molecular genetic research and metabolism. Thanks to the conserved cellular mechanisms between yeast and higher eukaryotes, which govern basic functions such as replication or cell division, *S. cerevisiae* serves as the perfect model to unravel the secrets behind eukaryotic life.

2. Alkaline pH adaptation of *S. cerevisiae*

Like many other organisms, fungi are subjected to changes in the environment that affect their capacity to grow and reproduce. Drastic changes in the external pH imply a profound alteration of the optimal growth conditions and trigger differentiation programs. The adaptation mechanisms to this stress were first documented in the filamentous fungi *Aspergillus nidulans* and the pathogen *Candida albicans*, where it was described that alkaline conditions entail a remodeling of the transcriptional profile. In the case of *A. nidulans,* it was observed that shifting from acidic to alkaline conditions prompted the repression of acid extracellular secreted enzymes (e.g. acid phosphatase) and the induction of alkaline versions of those enzymes (e.g. alkaline phosphatase) (Caddick *et al.*, 1986). In fungal pathogens such as *C. albicans* adaptation to a range of different pH is essential for virulence since it infects anatomical sites of diverse pH. It was described that this pathogen responds to external pH using it as a signal for morphological differentiation, adopting a yeast form under acidic conditions and favoring hyphal growth under alkaline ones (Davis, 2003). For more information on the alkaline response of these organisms see section 2.6.

The budding yeast can grow over a broad range of external pH, preferring acid conditions to neutral or alkaline. *S. cerevisiae* pumps protons out from its cytoplasm to some organelles, e.g. the vacuole, and to the external medium, acidifying its surroundings. This causes a relative internal alkalinization and generates a chemical proton gradient across the plasma membrane (Serrano *et al.*, 1986). The protein responsible for proton extrusion at the plasma membrane is Pma1, a P2-type ATPase which pumps one proton for every ATP hydrolyzed. Along with the vacuolar proton-translocating ATPase, which pumps protons into the vacuole, Pma1 helps maintain a cytosolic pH around 7 that is stable over a broad range of external pH (Martínez-Muñoz and Kane, 2008; Orij *et al.*, 2012). Secondary symporters and antiporters consume this gradient to uptake a wide variety of nutrients, ranging from ions (mainly potassium) to amino acids or sugars, making this gradient essential for cell survival and proliferation.

External alkalinization disrupts the electrochemical gradient impairing proper transport across the plasma membrane, thus it generates a stressful situation the cells must cope with. Over the last decade the response of *S. cerevisiae* to an alkaline pH stress has been thoroughly studied, pointing out its diversity and complexity. Genome-wide approximations and identification of mutant strains with an altered growth under high pH conditions has demonstrated that this particular stress has a wide impact on the cell's physiology, as it can be inferred by the numerous pathways involved in the response (Figure 1) (Casado *et al.*, 2011; Hong and Carlson, 2007; Lamb *et al.*, 2001; Serrano *et al.*, 2002, 2004; Serra-Cardona *et al.*, 2015).

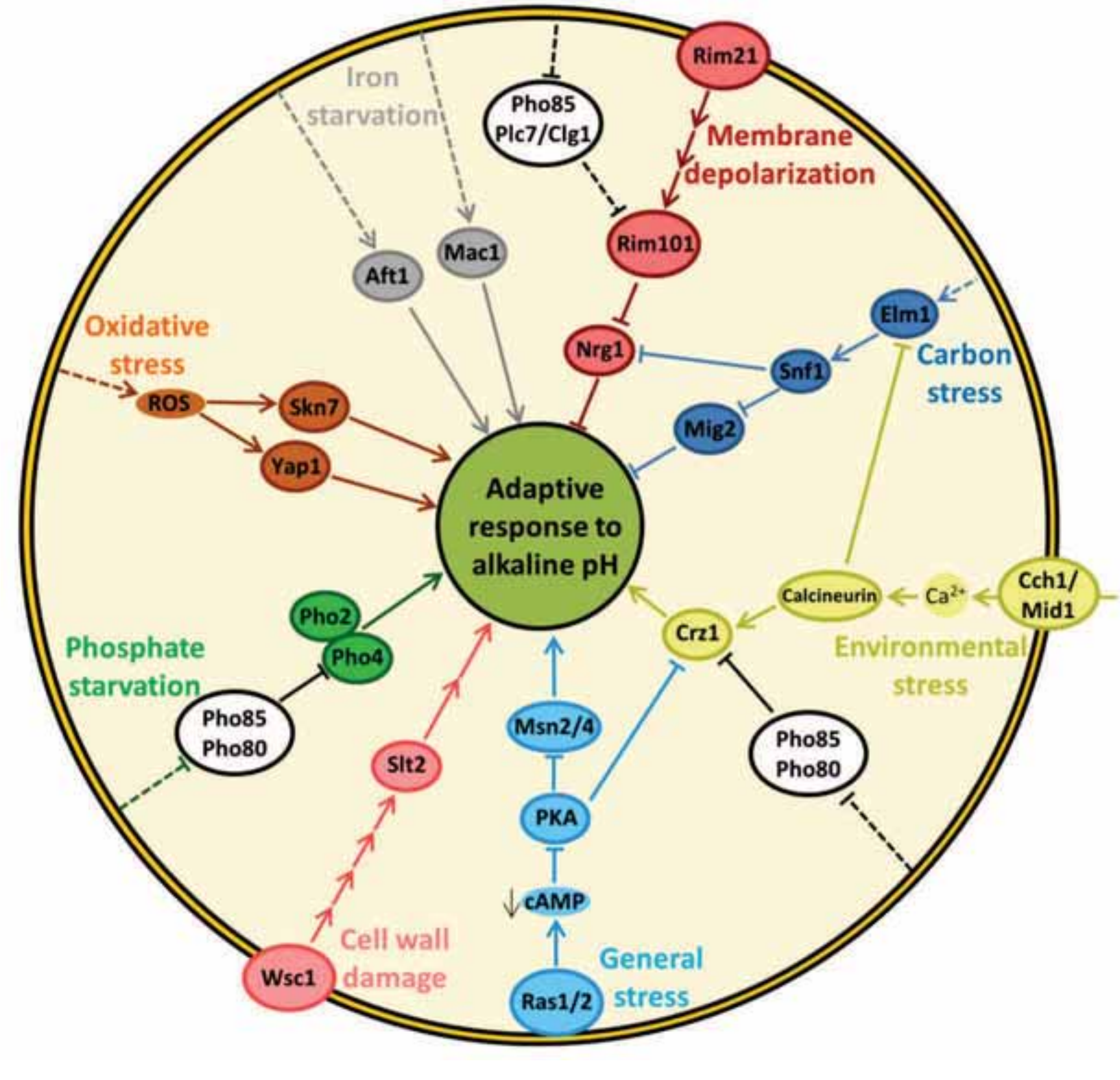
Iron starvation
Pho85
Plc7/Clg1
Rim21
Membrane depolarization
Rim101
Mac1
Aft1
Oxidative stress
ROS
Skn7
Yap1
Nrg1
Elm1
Snf1
Mig2
Carbon stress
Adaptive response to alkaline pH
Calcineurin
Ca2+
Cch1/Mid1
Crz1
Environmental stress
Pho2
Pho4
Phosphate starvation
Pho85
Pho80
Slt2
Msn2/4
PKA
cAMP
Pho85
Pho80
Cell wall damage
Wsc1
Ras1/2
General stress

Figure 1. Simplified representation of the different pathways driving the adaptive response to alkaline pH stress and the interactions between them. Each pathway will be discussed below in their own section.

The activation of these pathways leads to a complex remodeling of the gene expression, repressing those genes whose products are not necessary or might have a detrimental effect under high pH conditions and inducing those necessary for adaptation. Interestingly, the response to alkaline conditions largely includes the transcriptional changes observed in the starvation responses for different nutrients, namely glucose, phosphate, or iron/copper (Lamb *et al.*, 2001; Serrano *et al.*, 2004; Viladevall *et al.*, 2004), indicating a general impairment in nutrient transport and/or utilization.

2.1. The Rim101 pathway

S. cerevisiae Rim101 was first identified as a positive regulator of meiosis and sporulation, inducing the expression of *IME2* through *IME1* (Su and Mitchell, 1993a). Later on, due to its similarities with the previously characterized transcription factor PacC of *A. nidulans*, it was determined that Rim101 was implicated in the adaptation to alkaline conditions (Lamb *et al.*, 2001; Li and Mitchell, 1997).

THE RIM101 SIGNALING CASCADE

The Rim101 pathway triggers the activation of the Rim101 transcription factor by C-terminal proteolytic cleavage and it is comprised of seven components: Rim8, Rim9, Rim13, Rim20, Rim21, Dfg16, and Ygr122w, all of them required for the correct proteolysis of Rim101 by Rim13 (Figure 2). Signaling starts at the plasma membrane, and involves the 7 transmembrane protein Rim21 and its homologue Dfg16, and the 3 transmembrane protein Rim9 (Barwell *et al.*, 2005; Denison *et al.*, 1998; Tréton *et al.*, 2000). A depolarization of the plasma membrane, caused either by external alkalinization or other mechanisms, triggers signaling in a Rim21-dependent manner, relegating Dfg16 and Rim9 to auxiliary functions like proper accumulation and localization of Rim21 (Obara *et al.*, 2012). Because of the internalization of these three proteins upon external alkalinization and the requirement of some factors involved in the endosomal sorting complex required for transport (ESCRT), it was believed that the pH signal was transduced to internal compartments (Xu *et al.*, 2004). However, it was reported recently that, after the alkaline stimulus, downstream proteins Rim8, Rim13, and Rim20 are recruited at the plasma membrane, as well as the ESCRT-III protein Snf7, in a Rim21-dependent fashion (Obara and Kihara, 2014).

Assembly of all these factors permits the interaction between Rim20 and the PEST-like sequence of Rim101 and between the Bro1-domain of Rim20 and Snf7, which associates with the calpain-like cysteine protease Rim13 (Ito *et al.*, 2001). This provides a scaffold for Rim13 to perform the proteolytic cleavage of Rim101 (Futai *et al.*, 1999; Xu and Mitchell, 2001). Rim8, an α–arrestin known to bind to Rim21, also interacts with the ESCRT-I factor Stp22, providing a putative link between the sensing complex and the proteolytic complex via the ESCRT machinery (Herrador *et al.*, 2010). Rim8 is ubiquitinated by the E3 ubiquitin ligase Rsp5 independently of ambient pH and this process is not essential for signaling (Herrador *et al.*, 2010). However, the activity of Rsp5 is necessary for activation of the Rim101 pathway, indicating the existence of unknown targets whose ubiquitination is required for Rim101 proteolysis (Obara and Kihara, 2014). Although its function is not clear, Ygr122w, like Rim20, also contains a Bro1-domain and interacts with Snf7, probably being an additional member of the Rim20-Snf7 scaffold (Rothfels *et al.*, 2005).

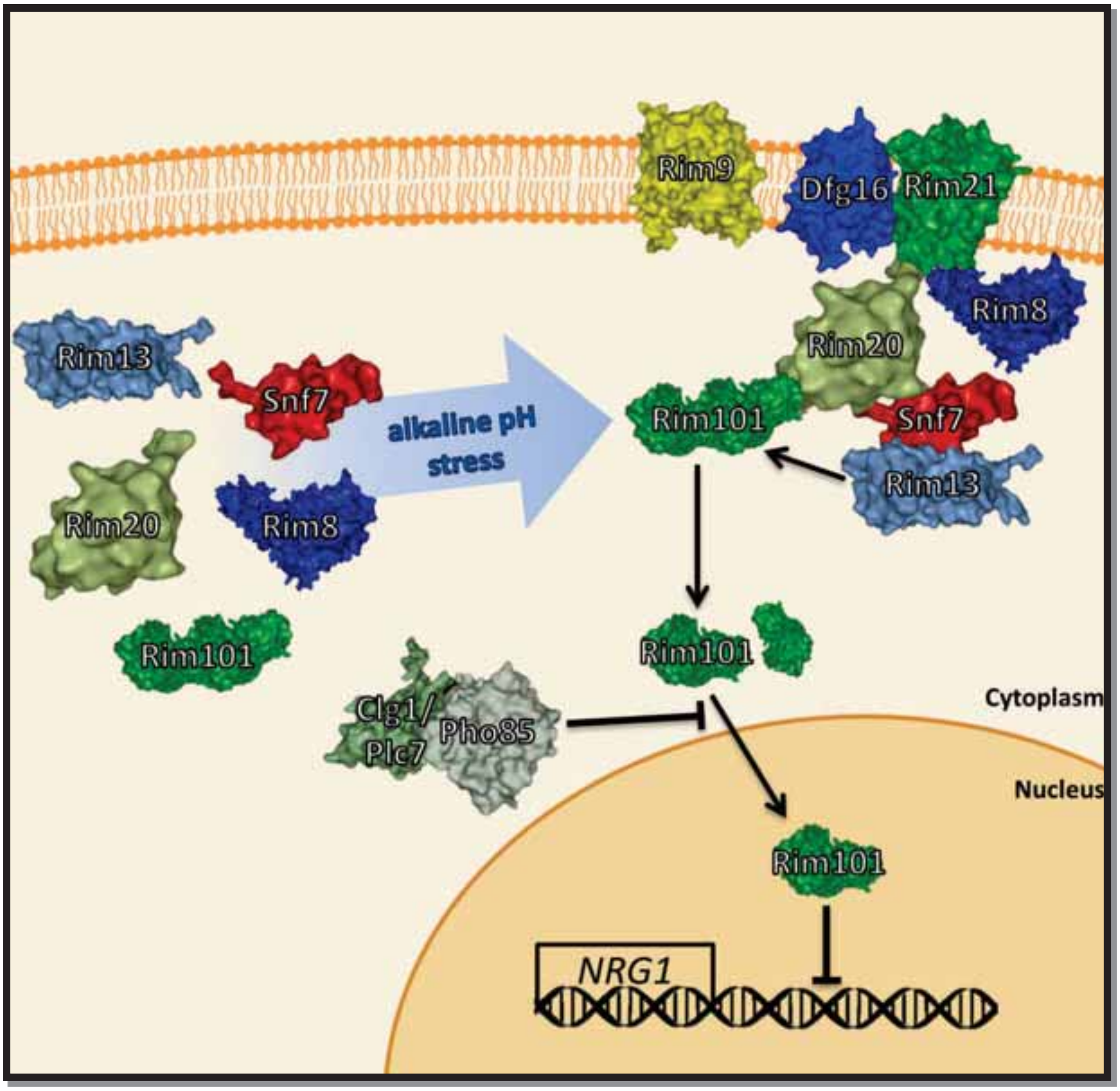
Rim9
Dfg16
Rim21
Rim8
Rim13
Snf7
Rim20
alkaline pH stress
Rim101
Rim20
Snf7
Rim8
Rim13
Rim101
Rim101
Clg1/Plc7
Pho85
Cytoplasm
Nucleus
Rim101
NRG1

Figure 2. Representation of the Rim101 pathway depicting the assembly of its components upon alkaline stress. As shown, Rim21 triggers the signaling cascade which ultimately leads to the interaction between Rim13 and Rim101, causing the proteolysis of the latter and its subsequent translocation to the nucleus.

Rim101 regulation

Rim101 is a 628-residue protein with three C_2H_2 zinc finger domains essential for its function (Su and Mitchell, 1993b). The activation of the Rim101 pathway leads to a C-terminal proteolytic cleavage generating the active form of Rim101, 100-residue shorter than its inactive version (Li and Mitchell, 1997). The loss of some members of the pathway, like Rim8, Rim9, or Rim13, impairs the activation of Rim101, causing a phenotype that can be suppressed by expression of a truncated version of Rim101, equivalent to its active form (Li and Mitchell, 1997). Apart from being regulated by proteolysis, it was reported that Rim101 localization was controlled by the cyclin-dependent kinase (CDK) Pho85. This protein, in association with cyclins Plc7 or Clg1, would be phosphorylating both versions of Rim101 and promoting their nuclear exclusion (Nishizawa *et al.*, 2010). The authors speculated that phosphorylation could increase its affinity for the exportin Msn5. To note that Pho85 has a broad role in adaptation to environmental stress, especially alkaline pH stress.

Rim101 function in alkaline and salt stress

As mentioned above, Rim101 is a transcription factor with a relevant function in high pH stress adaptation. This became evident with the observation that the absence of Rim101 or some members of its pathway led to a sensitivity phenotype under alkaline conditions (Futai *et al.*, 1999; Lamb *et al.*, 2001). This transcription factor governs the expression under alkaline pH stress of several genes, including the siderophore-iron transporter *ARN4* and the vacuolar H^+-ATPase subunit *VMA4* (Lamb *et al.*, 2001). It is also partially responsible for the induction of the expression of the Na^+-ATPase-encoding gene *ENA1*, the low-affinity iron transporter *FET4*, and the transcriptional repressor *NRG2*. This regulation is performed indirectly, since Rim101 is a transcriptional repressor of *NRG1* and *SMP1* (Lamb and Mitchell, 2003). Nrg1, also a transcriptional repressor, blocks the transcription of several genes, like *ENA1*; thus, activating Rim101 prompts the expression of *ENA1* through repression of *NRG1*. This explains why the loss of *NRG1* in a strain lacking *RIM101* restores growth at both alkaline pH and high concentrations of Na^+, and reestablishes *ENA1* expression levels (Lamb and Mitchell, 2003). Both Nrg1 and its homologue Nrg2 were first identified as negative regulators of several glucose repressed genes such as *STA1*, *SUC2*, *DOG2*, and *GAL1* (Park *et al.*, 1999; Vyas *et al.*, 2001; Zhou and Winston, 2001) and as inhibitors of haploid invasive growth by repressing the expression of the cell surface glycoprotein-encoding gene *FLO11* in the presence of glucose (Kuchin *et al.*, 2002). These functions are negatively regulated by the Snf1 kinase, also related to the response to alkaline stress conditions (see section 2.3). Although Nrg1 and Nrg2 control the expression of a similar set of genes, their regulation at the RNA and protein levels differ considerably under certain situations, like glucose limitation or growth in non-fermentable carbon sources (Berkey *et al.*, 2004).

The transcription factor Smp1, also repressed by Rim101, is not involved in alkaline pH tolerance or *ENA1* expression (a strain lacking *RIM101* and *SMP1* does not return to normal tolerance to high pH nor *ENA1* expression levels). On the other hand, Smp1 plays a role in meiosis and sporulation: the *smp1* mutation suppressed the *rim101* mutant defect in invasive growth and sporulation (Lamb and Mitchell, 2003). This suggests that Smp1 is negatively regulating these processes. Smp1 also participates in the response to osmotic stress by activating the transcription of some osmoresponsive genes (de Nadal *et al.*, 2003). As it will be discussed later (section 2.4), alkaline pH treatment activates the protein kinase C (Pkc1)-Slt2 pathway, responsible for cell wall remodeling and integrity (CWI). Under high pH stress, the Rim101 pathway acts in parallel with the CWI Slt2 pathway. In fact, the absence of both Rim101 and Slt2 proteins is synthetically lethal in non-osmotically stabilized media (Castrejon *et al.*, 2006). It was reported that Rim101 may retain some functionality at acid conditions: this transcription factor is involved in the resistance to weak organic acids at pH 4 by contributing to cell wall remodeling and proper acidification of the vacuole (Mira *et al.*, 2009). The role of Rim101 in vacuole acidification has also been related to resistance to low concentrations of the oxidant selenite: the derepression of V-ATPase genes by Rim101, such as *VMA2*, would help to maintain correct vacuolar function needed to fight against selenite (Pérez-Sampietro and Herrero, 2014).

2.2. The calcineurin pathway

Calcineurin, or protein phosphatase 2B, is a serine/threonine phosphatase highly conserved among eukaryotes. A wide variety of stimuli cause transitory increases of cytosolic calcium, leading to the activation of the Ca^{2+}–binding protein calmodulin which in turn activates calcineurin (Cyert, 2001). In mammals, calcineurin participates in many different processes, from dephosphorylating the NFAT transcription factor during T-lymphocytes activation to regulating insulin secretion (Rusnak and Mertz, 2000).

In *S. cerevisiae* calcineurin is a heterodimer comprised of one of the two redundant catalytic subunits Cna1 or Cna2 and the regulatory subunit Cnb1 (Cyert and Thorner, 1992; Cyert *et al.*, 1991). Although it is dispensable for growth under standard culture conditions, it becomes essential when cells are exposed to more stringent situations. The activity of the budding yeast calcineurin was first related to growth restoration after exposure to the mating pheromone (Cyert *et al.*, 1991) but further studies revealed its involvement with other conditions that triggered an increase of cytosolic calcium. Some examples are elevated concentrations of sodium, lithium, or manganese (Farcasanu *et al.*, 1995; Mendoza *et al.*, 1994; Nakamura *et al.*, 1993), hypotonic shock (Batiza *et al.*, 1996), high temperature (Zhao *et al.*, 1998), or cell wall damage (Zakrzewska *et al.*, 2005). Calcineurin was also connected with the response to high pH when it was observed that the expression of some genes after an alkaline treatment was dependent on this phosphatase (Serrano *et al.*, 2002).

CALCINEURIN REGULATION

Calcium distribution in the different cellular compartments is tightly regulated: a low cytosolic concentration must be maintained in order to use this ion as a signal, thus it must be stored in other organelles (Dunn *et al.*, 1994; Iida *et al.*, 1990). The main reservoir is the vacuole, accounting for more than 90% of the total calcium (Dunn *et al.*, 1994), and the rest is stored in the endoplasmic reticulum and Golgi. The budding yeast possesses two mechanisms for Ca^{2+} influx across the plasma membrane: the high-affinity system, comprised of the transmembrane proteins Mid1 and Cch1 (Iida *et al.*, 1994; Paidhungat and Garrett, 1997) and their putative regulatory subunit Ecm7 (Figure 3)(Martin *et al.*, 2011), and the low-affinity system, less well-defined and activated in the presence of high concentrations of pheromone (Muller *et al.*, 2003). Additionally, vacuolar transporters Pmc1 and Vcx1 mediate calcium influx into the vacuole, maintaining a low cytosolic concentration of this ion (Cunningham and Fink, 1994, 1996). The cytosolic calcium needed to activate calcineurin may come from the intracellular compartments or the external medium, depending on the stimulus. For example, it was reported that during an osmotic shock Ca^{2+} is released from the vacuole through the calcium channel Yvc1 (Denis and Cyert, 2002; Palmer *et al.*, 2001) but it also enters from the extracellular medium through Mid1/Cch1 (Matsumoto *et al.*, 2002). In other cases, such as alkaline or endoplasmic reticulum stress, calcineurin activation depends exclusively on external calcium and Mid1/Cch1 function (Bonilla *et al.*, 2002; Viladevall *et al.*, 2004). Although the exact mechanism of Mid1/Cch1 activation is not fully understood, it was proposed that Mid1 may be mechanosensitive (Kanzaki *et al.*, 1999) while Cch1 could be voltage-gated (Paidhungat and Garrett, 1997), which would explain the relationship between the activation of the calcineurin pathway and certain environmental stresses.

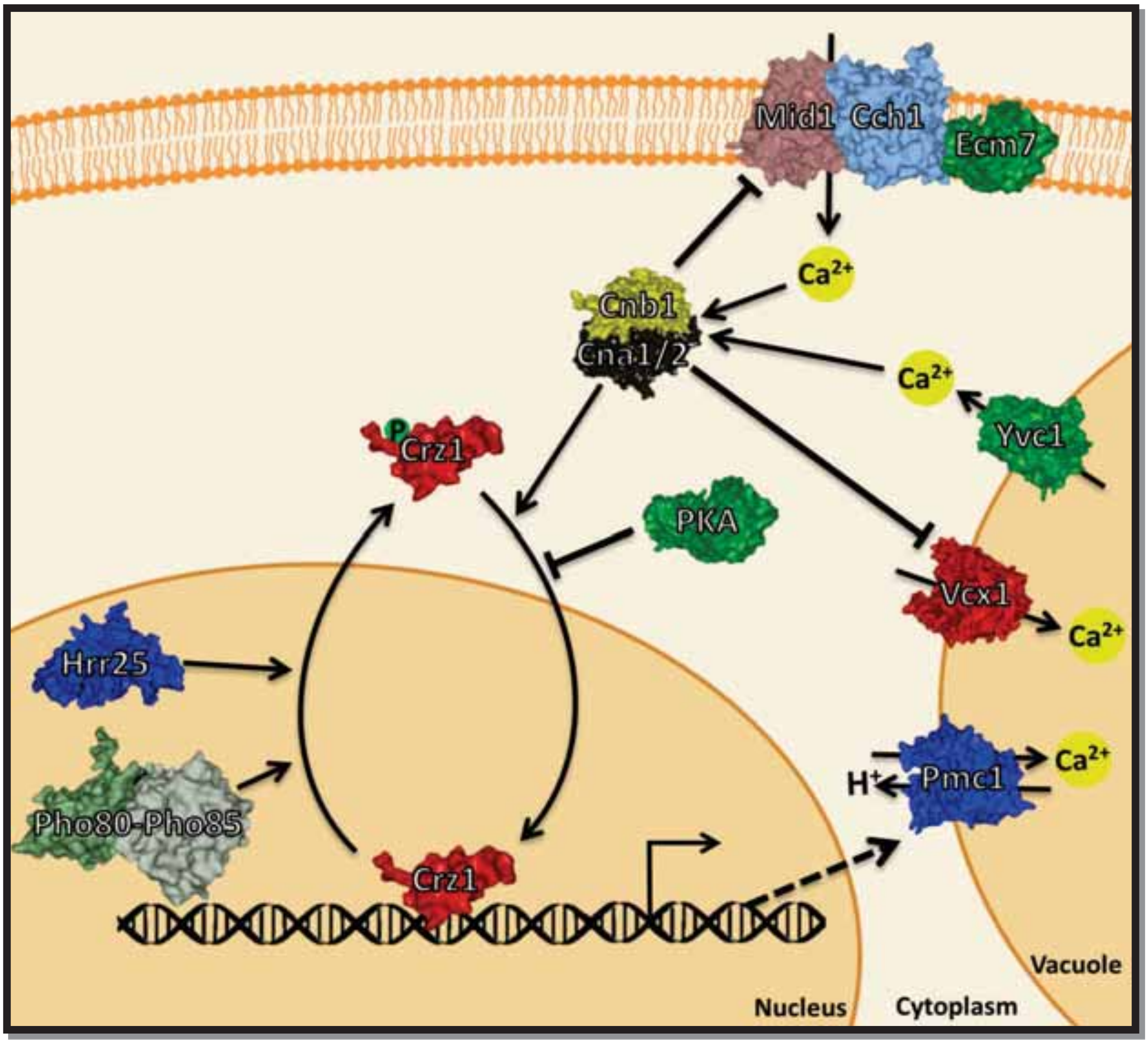

Figure 3. Schematic illustration of the calcineurin pathway. Cytosolic calcium activates calcineurin, comprised of Cnb1 and Cna1 or Cna2. Calcineurin regulates the activity of the calcium channels Mid1 and Vcx1 and the localization of Crz1, prompting its nuclear import. One of the gene products induced by Crz1, Pmc1, is also involved in calcium homeostasis.

Apart from the Ca^{2+} concentration, calcineurin is also regulated by the calcipressin Rcn1: when phosphorylated by Mck1, Rcn1 activates calcineurin. Rcn1 is in turn dephosphorylated by calcineurin itself, providing a complex regulatory feedback of calcineurin activity (Hilioti *et al.*, 2004). It is worth mentioning that the activation of the calcineurin signaling pathway also induces *RCN1* transcription (Hilioti *et al.*, 2004). Furthermore, by activating the transcription of *PMC1*, the gene encoding the vacuolar Ca^{2+} ATPase, and regulating Mid1/Cch1 and Vcx1 activity, calcineurin controls the cytosolic calcium concentration which may affect its own activity (Bonilla and Cunningham, 2003; Cunningham and Fink, 1994; Pittman *et al.*, 2004).

Calcineurin function

Calcineurin recognizes the small docking sites PxIxIT and LxVP in its substrates, and the calcineurin inhibitors FK506 and cyclosporine A act as such by blocking substrate binding at these sites (Roy and Cyert, 2009). Calcineurin best-known substrate is the zinc-finger transcription factor Crz1. When cytosolic calcium increases, calcineurin becomes activated and dephosphorylates Crz1 (Matheos *et al.*, 1997; Stathopoulos and Cyert, 1997). By binding to the karyopherin Nmd5, the dephosphorylated form of Crz1 can enter the nucleus where it recognizes the calcineurin-dependent response elements (CDREs) of different promoters to activate their transcription (Polizotto and Cyert, 2001; Stathopoulos and Cyert, 1997). Under non-stressing conditions calcineurin is inactive and Crz1 exists in a phosphorylated state, which prompts its nuclear exclusion by binding to the Msn5 exportin (Boustany and Cyert, 2002). Three different kinases have been described to phosphorylate Crz1: Hrr25 (Kafadar *et al.*, 2003), protein kinase A (PKA)(Kafadar and Cyert, 2004) and the Pho80-Pho85 complex (Sopko *et al.*, 2006)(Figure 3). While Hrr25 and Pho80-Pho85 phosphorylation promotes Crz1 nuclear exclusion, phosphorylation by PKA would inhibit nuclear import (Kafadar and Cyert, 2004). Apart from its influence on Crz1, both Pho85 and PKA play other significant roles in the response to a high pH stress (see section 2.4 and 3).

A DNA microarray experiment identified more than 160 genes whose expression in response to high concentrations of Ca^{2+} or Na^{+} was calcineurin-dependent (Yoshimoto *et al.*, 2002). Among them were genes related to small molecule transport, ion homeostasis, and cell wall maintenance and most of them relied on Crz1 for induction. Under alkaline conditions, calcineurin/Crz1 becomes essential for the expression of some genes such as the Na^{+}-ATPase *ENA1* or the Na^{+}/phosphate co-transporter *PHO89* (Serrano *et al.*, 2002). Further studies revealed that high pH stress results in a fast and transient calcium burst from the external medium to the cytoplasm mediated by Mid1/Cch1, triggering a calcineurin-mediated response (Viladevall *et al.*, 2004). This rise in calcium concentration becomes apparent at pH 7.5 and increases until pH 8.2, following the same profile as *PHO89* induction under these same circumstances (Serrano *et al.*, 2002). The calcineurin-dependent genes account for 10% of the total genes induced under an alkaline stress and most of them are induced in the early stages of the alkaline pH response, in agreement with the described calcium kinetics (Viladevall *et al.*, 2004). As it was observed in the presence of high levels of external calcium, most of the transcriptional response mediated by calcineurin under alkaline conditions is Crz1-dependent. This same pathway also participates in the induction of several genes required for the glucose starvation response and some of them, such as the high-affinity glucose transporter-encoding gene *HXT2*, require both the calcineurin/Crz1 and the Snf1 pathway to be fully induced under alkaline conditions (Ruiz *et al.*, 2008). In fact, the growth defect of a *snf1* mutant strain in low glucose conditions can be overridden by the addition of external calcium, implying that calcineurin activation is sufficient to restore the expression of the Snf1-dependent glucose repressed genes (Ruiz *et al.*, 2008).

Even though Crz1 plays a central role in the response driven by calcineurin, this phosphatase has other substrates through which it controls different processes. This can be inferred from the higher sensibility to Mn^{2+} and Li^{+} ions and to alkaline pH displayed by the *cnb1* mutant strain when compared to the *crz1* mutant strain (Stathopoulos and Cyert, 1997), suggesting that other targets of calcineurin must participate in the response to these straining situations. For instance, calcineurin activates by dephosphorylation the tail-anchored endoplasmic reticulum membrane protein Hph1 (Heath *et al.*, 2004). Cells lacking both Hph1 and its homolog Hph2 (renamed as Ftr1 and Frt2) show impaired growth under conditions of high salinity, high pH, and cell wall stress, pointing toward a Crz1-independent function of calcineurin in the response to these stresses (Heath *et al.*, 2004). A recent work found that Hph1 and Hph2 interacted with the Sec63/Sec62 complex, which is involved in the posttranslational translocation of proteins, promoting vacuolar proton-translocating ATPase biogenesis (Piña *et al.*, 2011). An impaired vacuolar ATPase activity, with the subsequent deficiency in vacuolar acidification, would explain the alkali-sensitivity displayed by the *hph1 hph2* and *cnb1* mutant strains.

Calcineurin activity has also been linked with cell cycle blockage. It was observed that calcineurin upregulates the transcription of *SWE1*, encoding a negative regulator of cell cycle progression, and promotes the degradation of Hsl1 and Yap1 by dephosphorylating them, delaying the transition between G_2 to M phase (Mizunuma *et al.*, 1998, 2001; Yokoyama *et al.*, 2006). In a recent report the Elm1 protein kinase was identified as a substrate of calcineurin, revealing that dephosphorylation of Elm1 reduces its activity and impairs progression through G_1 phase (Goldman *et al.*, 2014). Interestingly, during an alkaline pH stress, Elm1 activates the Snf1 kinase to promote transcription of several genes (see section 2.3), some of them in conjunction with Crz1 (Casamayor *et al.*, 2012; Ruiz *et al.*, 2008). Thus, under alkaline conditions, calcineurin would be activating the transcription of some target genes via Crz1 while attenuating their induction through Elm1 inhibition. The multiple calcineurin targets oriented to delay cell cycle progression may be a mechanism for the cell to have enough time, when confronted with a straining situation, for the adaptive response to take effect before resuming proliferation.

2.3. The Snf1 pathway

The adenosine monophosphate-activated protein kinase (AMPK) is an enzyme involved in cellular energy homeostasis conserved among eukaryotes. Its main role is to sense and respond to the energy status of the cell in terms of the AMP:ATP ratio: when this ratio increases, meaning a low energy status, AMPK becomes activated driving a response to increase ATP synthesis and decrease its consumption (Hardie, 2011). Additionally, it has been related to mitochondria biogenesis and disposal, proliferation, and cell polarity (Hardie, 2011).

In *S. cerevisiae* the gene encoding the AMPK homologue is *SNF1,* first identified as an essential locus for the utilization of non-fermentable carbon sources (Carlson *et al.*, 1981). It was found that, in the absence of glucose, Snf1 triggered the expression of genes needed for the consumption of alternative carbon sources, normally repressed by glucose. One example is the *SUC2* gene, encoding an invertase required for sucrose utilization, whose secreted (active) form is glucose-repressed and becomes derepressed upon activation of Snf1 (Carlson and Botstein, 1982). Further works identified Snf1 as a serine/threonine protein kinase (Celenza and Carlson, 1986) and, apart from its role in expression of the glucose-repressed genes, it was linked to several other nutrient-responsive cellular processes. Some examples are meiosis and sporulation, by inducing *IME1* and *IME2* transcription (Honigberg and Lee, 1998), and haploid invasive growth, by regulating the transcription factors Sip4, Msn1, and Nrg1/Nrg2 (Cullen and Sprague, 2000; Kuchin *et al.*, 2002). In addition to drive the response to nutrient stresses, Snf1 also plays a role in adaptation to environmental stresses such as high concentrations of Na^+, oxidative stress, or alkaline pH (Alepuz *et al.*, 1997; Hong and Carlson, 2007; Platara *et al.*, 2006).

STRUCTURE OF THE SNF1 COMPLEX

The SNF1 complex is a heterotrimer comprised of the catalytic α subunit Snf1, three alternate β subunits (Sip1, Sip2, and Gal83) and the γ subunit Snf4. The Snf1 subunit contains a kinase domain in the N-terminal region and a regulatory domain in the C-terminal region (Celenza and Carlson, 1986, 1989). The first role attributed to the β subunits Sip1, Sip2, and Gal83 was as anchors to form the SNF1 complex by binding to Snf1 and Snf4 (Jiang and Carlson, 1997). Later it was discovered that the three β subunits are not redundant and each one of them direct the SNF1 complex to different targets (Schmidt and McCartney, 2000). This target specialization is achieved by regulating Snf1 subcellular localization: upon glucose depletion, the β subunits translocate to different cell compartments directing the kinase activity to specific substrates (Vincent *et al.*, 2001). Gal83 is the most abundant β subunit so, as expected, it is the major subunit driving SNF1 activity in response to glucose limitation (Hedbacker *et al.*, 2004a). The levels of Sip2, the second β subunit in abundance, increase in response to the presence of non-fermentable carbon sources, and Sip1 is the least abundant (Ghaemmaghami *et al.*, 2003; Vincent *et al.*, 2001).

REGULATION OF SNF1 CATALYTIC ACTIVITY

The main factor regulating Snf1 catalytic activity is phosphorylation of its Thr210 in the catalytic domain and this phosphorylation serves as the mechanism by which upstream kinases and phosphatases regulate SNF1 activity (McCartney and Schmidt, 2001). Even though Thr210 phosphorylation correlates with a high AMP:ATP ratio, SNF1 is not allosterically activated by AMP *in vitro*, as opposed to other eukaryotic AMPKs (Mitchelhill *et al.*, 1994; Wilson *et al.*, 1996; Woods *et al.*, 1994). Actually, it was recently discovered that SNF1 is regulated by ADP: when ADP binds to Snf4, the γ subunit exerts a protective effect against the dephosphorylation of Thr210 (Mayer *et al.*, 2011). The regulatory domain exerts another layer of regulation: in the presence of glucose, it binds to the catalytic domain, producing an autoinhibitory effect of the kinase activity. However, under low glucose conditions, the γ subunit Snf4 is bound to the regulatory domain, counteracting autoinhibition (Jiang and Carlson, 1996). Phosphorylation of Thr210 occurs under several conditions, such as glucose limitation, nitrogen limitation, sodium ion stress, or alkaline pH (Hong and Carlson, 2007; McCartney and Schmidt, 2001; Orlova *et al.*, 2006). Interestingly, this activation is often transient: while SNF1 activity is rapidly elevated when cells are shifted from glucose to sucrose containing medium, after adaptation its activity returns to basal levels (Hedbacker and Carlson, 2006). Similarly, after an alkaline pH stress, SNF1 activity increase within 5 minutes but is reduced to basal levels after 1 hour (Hong and Carlson, 2007).

The upstream kinases responsible for Thr210 phosphorylation are Sak1, Elm1, and Tos3 (Figure 4)(Hong *et al.*, 2003). They are highly similar but, in most of the cases, Sak1 is the major Snf1-activating kinase (Hong and Carlson, 2007; McCartney *et al.*, 2005). There is no evidence for their activity being regulated by glucose signals, and the β subunit of the SNF1 complex determines the preference for each upstream kinase (McCartney *et al.*, 2005). Under some circumstances, such as utilization of carbon sources other than glucose, Sak1, Elm1, and Tos3 are functionally redundant, as indicated by the need to mutate all three to confer the *snf1* phenotype (Hong *et al.*, 2003). However, this is not the case for adaptation to alkaline pH: the *elm1* mutant strain displays a strong alkali-sensitive phenotype while the absence of the Sak1 and/or Tos3 does not affect growth under this condition (Casamayor *et al.*, 2012). Although the *elm1* phenotype is not as strong as the *snf1* phenotype, it indicates that Elm1 is the major kinase triggering the Snf1-mediated response to a high pH stress. Notably, the triple *sak1 elm1 tos3* mutation shows an even more pronounced phenotype than the *snf1* mutation, suggesting other important roles for these kinases in high pH tolerance besides Snf1 regulation (Casamayor *et al.*, 2012). It is worth considering that the *elm1* mutation may impinge on Snf1-independent processes such as progression through G_1 phase or the G_2/M morphogenesis checkpoint (Sreenivasan *et al.*, 2003; Szkotnicki *et al.*, 2008). In this regard, Elm1 dephosphorylation by calcineurin would be one of the mechanisms by which the phosphatase delays cell cycle progression, as mentioned in section 2.2 (Goldman *et al.*, 2014).

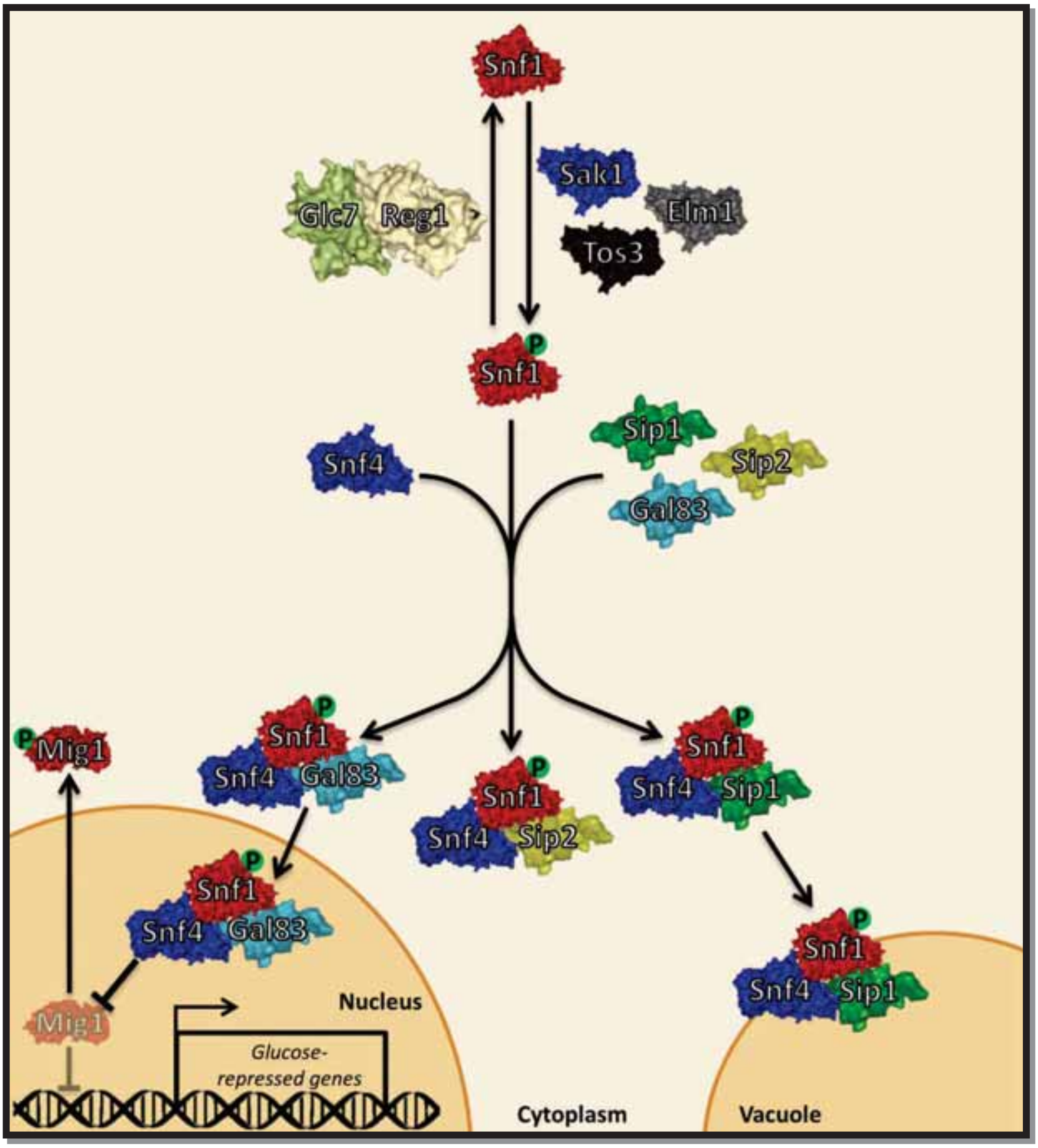
Snf1
Sak1
Glc7
Reg1
Elm1
Tos3
P
Snf1
Sip1
Snf4
Sip2
Gal83
P
Mig1
P
Snf1
Snf4
Gal83
P
Snf1
Snf4
Sip2
P
Snf1
Snf4
Sip1
P
Snf1
Snf4
Gal83
Mig1
Nucleus
Glucose-
repressed genes
P
Snf1
Snf4
Sip1
Cytoplasm
Vacuole

Figure 4. Representation of the Snf1 pathway. Snf1, when phosphorylated by Sak1, Elm1, or Tos3, forms the SNF1 complex in association with Snf4 and one β subunit. Sip1 directs the complex to the vacuole while Sip2-Snf4-Snf1 remains cytosolic. Gal83 drives the complex into the nucleus, where it phosphorylates the transcriptional repressor Mig1 prompting its nuclear exclusion.

The Glc7-Reg1 protein phosphatase 1 (PP1) complex is the one responsible for glucose repression by dephosphorylating Snf1 Thr210 (Ludin *et al.*, 1998; McCartney and Schmidt, 2001; Tu and Carlson, 1995). The Reg1 regulatory subunit directs Glc7 catalytic activity to Snf1 by binding to both the kinase and the phosphatase (Sanz *et al.*, 2000). Snf1 activation causes Reg1 phosphorylation in a Snf1-dependent manner, which releases Reg1 from the kinase complex preventing further inactivation by PP1 (Sanz *et al.*, 2000). As expected, the absence of Reg1 abolishes glucose inhibition of Snf1, which becomes active when cells are grown with glucose as the carbon source (Hong *et al.*, 2005). Since both the upstream kinases and PP1 are catalytically active regardless of glucose availability, it was hypothesized that the glucose signal regulates the exposure of the Thr210 through an unknown factor, which would protect it from dephosphorylation in low glucose conditions (Rubenstein *et al.*, 2008).

More recently other phosphatases have been associated with Snf1 inactivation. The phosphatase Sit4 contributes to Snf1 dephosphorylation since the *sit4* mutation exhibits Thr210 phosphorylation in the presence of glucose and Sit4 is physically associated with Snf1 (Ruiz *et al.*, 2011). Another case is the Ptc1 phosphatase which, like Sit4, has overlapping functions with Glc7-Reg1 in the glucose regulation of SNF1. These 3 phosphatases ensure that Snf1 Thr210 remains dephosphorylated in the presence of high concentrations of glucose, with Glc7-Reg1 playing a major role (Ruiz *et al.*, 2013).

REGULATION OF SNF1 SUBCELLULAR LOCALIZATION

SNF1 substrate specificity is also regulated by its subcellular localization, which is determined by the β subunit. In glucose-grown cells, the Snf1 subunit is localized in the cytoplasm, as well as the three β subunits are. However, when growing on alternative carbon sources, Sip1 translocates to the vacuole, Gal83 accumulates in the nucleus, and Sip2 remains cytoplasmic (Figure 4)(Vincent *et al.*, 2001). Moreover, this differential localization depends on their divergent N-terminal region (Hedbacker and Carlson, 2006; Hedbacker *et al.*, 2004b) and it determines Snf1 distribution (Vincent *et al.*, 2001). Even though sodium ion stress prompts Snf1 Thr210 phosphorylation it does not translocate this subunit to the nucleus. In contrast, under alkaline pH conditions, Snf1 shows a nuclear localization (Hong and Carlson, 2007).

Although not fully understood, some mechanisms regulating β subunits translocation have been described. For instance, Sip1 vacuolar localization is downregulated by PKA (Hedbacker *et al.*, 2004b), a pathway also involved in adaptation to alkaline pH stress (see section 2.4). Gal83 nuclear localization is regulated by Snf1 itself: a catalytically inactive Snf1 inhibits Gal83 nuclear accumulation, promoting the retention of inactive Snf1 in the cytoplasm (Hedbacker *et al.*, 2004a).

SNF1 ROLE IN CARBON STRESS ADAPTATION

SNF1 regulates several cellular processes such as the transcription of a large set of genes or the activity of metabolic enzymes. Under glucose-limiting conditions, SNF1 controls the expression of over 400 genes, many of them related to transcription and signal transduction, broadening the influence of this kinase (Young *et al.*, 2003). This is achieved by a direct effect on transcriptional activators, repressors, and chromatin (Hedges *et al.*, 1995; Lesage *et al.*, 1996; Lo *et al.*, 2001; Ostling and Ronne, 1998).

In the absence of glucose, SNF1 activity positively regulates several transcription factors known to induce essential genes required for growth on such conditions. One example is the transcription factor Cat8, which is transcriptionally and posttranslationally activated in a SNF1-dependent fashion (Hedges *et al.*, 1995; Randez-Gil *et al.*, 1997). Cat8 then promotes the expression of genes encoding proteins required for gluconeogenesis and the utilization of ethanol or lactate as carbon sources (Young *et al.*, 2003). Similarly, Sip4 is also phosphorylated by SNF1 and this transcription factor is then responsible for the expression of gluconeogenesis-related genes (Vincent and Carlson, 1998, 1999). Snf1 regulates the localization of the stress-responsive Msn2 transcription factor: Msn2 is translocated from the cytoplasm to the nucleus in response to glucose starvation, and this process is downregulated by Snf1 (Mayordomo *et al.*, 2002). Msn2 and Msn4 play an important role in the adaptive response to high pH stress, as described in section 2.4.

Another mechanism by which SNF1 regulates gene expression is by relieving glucose-mediated repression. In glucose-grown cells, the transcriptional repressor Mig1 recruits the corepressors Ssn6-Tup1 to the promoters of the glucose-repressed gens thus blocking their transcription (Treitel and Carlson, 1995; Tzamarias and Struhl, 1995). Under conditions of glucose scarcity, SNF1 phosphorylates Mig1 (Ostling and Ronne, 1998; Smith *et al.*, 1999; Treitel *et al.*, 1998) promoting its nuclear export (DeVit and Johnston, 1999; DeVit *et al.*, 1997) and alleviating the glucose-driven repression (Figure 4). These derepressed genes are related to hexose transport, gluconeogenesis, and utilization of carbon sources such as galactose or sucrose (Westholm *et al.*, 2008). Many of these genes are also repressed by Mig2, a homolog of Mig1 (Westholm *et al.*, 2008) but, despite this functional redundancy, its regulation is somewhat different. *MIG1* expression is glucose-repressed by Mig1 and Mig2 while *MIG2* expression is constitutive (Lutfiyya *et al.*, 1998). Mig1 and Mig2 share the same binding sequence but bind to it with different affinity. For instance, *SUC2* repression is dependent on these two repressors although Mig2 exerts a much lesser effect on its promoter (Lutfiyya and Johnston, 1996). Something similar happens on the *GAL1* promoter: in the presence of glucose, only Mig1 is bound to it but when cells are shifted to galactose as carbon source, SNF1 phosphorylates Mig1 excluding it from the nucleus. Under this same conditions, Mig2 is degraded in a SNF1-dependent manner to prevent its binding to the *GAL1* promoter and further repression of *GAL*-driven expression (Lim *et al.*, 2011). A third homolog of these repressors, Mig3, is known to recognize the same DNA sequences but it does not have a relevant effect on the expression of any of the genes regulated by Mig1 and Mig2 (Lutfiyya *et al.*, 1998). Instead, it was found that Mig3 inhibits transcription of *SIR2*, a gene encoding a histone deacetylase involved in gene silencing (Westholm *et al.*, 2008).

The repressors Nrg1 and Nrg2 are also regulated by SNF1 in the absence of glucose. They were found to interact with Snf1 although their phosphorylation could not be detected (Vyas *et al.*, 2001). Nrg1 and Nrg2 RNA and protein levels are differently regulated by this kinase. In the presence of high levels of glucose, Snf1 downregulates *NRG1* expression whereas in glucose-limiting conditions it induces *NRG2* expression (Berkey *et al.*, 2004). It is worth noting that the expression of these two repressors is also oppositely regulated by the Rim101 pathway under alkaline pH conditions (see section 2.1). Unlike Mig1, Nrg1 localization remained nuclear in the absence of glucose (Vyas *et al.*, 2001) and some evidence suggests that Snf1 might be positively regulating Nrg1 levels (Berkey *et al.*, 2004). Among the targets of Nrg1 and/or Nrg2 are several genes needed for growth in the presence of carbon sources other than glucose, such as *SUC2* and *GAL* genes, required for sucrose and galactose utilization, respectively (Zhou and Winston, 2001), or the glucoamylase *STA1*, required for starch saccharification (Park *et al.*, 1999). These repressors also inhibit transcription of the cell surface glycoprotein-encoding gene *FLO11*, involved in haploid invasive growth (Kuchin *et al.*, 2002), and several stress-responsive genes, as discussed below.

Apart from its influence on transcription factors, SNF1 regulates gene expression by directly affecting the transcriptional apparatus or by chromatin remodeling. The expression of *INO1*, encoding an inositol-3-phosphate synthase, depends on Snf1 to recruit the TATA-binding protein on its promoter in the absence of inositol (Shirra *et al.*, 2005). Snf1 was also found to phosphorylate histone H3 Ser10 in vitro, which was related to age-associated gene desilencing (Lin *et al.*, 2003).

SNF1 is able to regulate the protein level of at least one target gene by controlling both its transcription and its protein stability. The expression of the lactate transporter-encoding gene *JEN1* is induced by Snf1 through inhibition of Mig1 and Mig2 and activation of Cat8 (Haurie *et al.*, 2000; Westholm *et al.*, 2008). In glucose-grown cells, the Glc7-Reg1 phosphatase dephosphorylates the arrestin-like protein Rod1, activating it and thereby promoting Jen1 endocytosis (Becuwe *et al.*, 2012). In contrast, when growing on lactate as carbon source, Snf1 phosphorylates Rod1, inhibiting its activity and thus keeping Jen1 from being degraded (Becuwe *et al.*, 2012).

Part of the SNF1-mediated response to carbon stress involves regulating the activity of metabolic enzymes. Under low glucose conditions, Snf1 phosphorylates and inactivates the acetyl-CoA carboxylase Acc1, thus favoring the accumulation of acetyl-CoA and inhibiting fatty acid biosynthesis (Mitchelhill *et al.*, 1994; Woods *et al.*, 1994). Snf1 also regulates the phosphorylation state of the glycogen synthase Gsy2, promoting glycogen accumulation (Hardy *et al.*, 1994). Interestingly, PKA and Pho85 antagonize Snf1 in regard of Gsy2 activity and glycogen accumulation (Hardy *et al.*, 1994; Huang *et al.*, 1996).

SNF1 ROLE IN ENVIRONMENTAL STRESS ADAPTATION

The Snf1 protein kinase is related to adaptation to several environmental stresses as demonstrated by the sensitivity of the *snf1* mutant strain to high concentrations of Na^+ or Li^+, oxidative stress, alkaline pH, and genotoxic stress by hydroxyurea, methyl-methane sulfonate, or cadmium (Alepuz *et al.*, 1997; Dubacq *et al.*, 2004; Hong and Carlson, 2007; Platara *et al.*, 2006), among others. The Snf1-mediated response to these situations varies with each stress although it often implies transcriptional regulation.

Surprisingly, resistance to hydroxyurea requires only residual Snf1 kinase activity even though Snf1-dependent phosphorylation of Mig3 is required to cope with this stress (Dubacq *et al.*, 2004). Similarly, despite the lack of Snf1 confers heat shock sensitivity, heat shock stress causes neither Snf1 Thr210 phosphorylation nor increase of Snf1 activity (Hong and Carlson, 2007). The same happens in the presence of a high concentration of cadmium: only basal levels of Snf1 activity are required and the Snf1-mediated resistance to this metal is independent of Mig1 (Thorsen *et al.*, 2009). Snf1 also participates in the adaptation to the presence of selenite, an agent that causes oxidative and DNA damage: Snf1 helps to maintain an adequate concentration of reduced glutathione to cope with this stress, and basal levels of Snf1 activity are enough for this protective role (Pérez-Sampietro *et al.*, 2013). In addition, the non-phosphorylated form of Snf1 is capable of mediating resistance to toxic cations through the upregulation of the potassium transporter Trk1, an indirect processes probably involving Sip4 (Portillo *et al.*, 2005).

In contrast, other environmental stresses lead to full activation of Snf1 by phosphorylation. Both salt and alkaline pH stress cause a fast increase in Snf1 phosphorylation as well as in its activity, but only in the case of salt stress this activity remained high one hour after the stress induction (Hong and Carlson, 2007; Ye *et al.*, 2008). As opposite to alkaline pH conditions, under salt stress Snf1 does not localize to the nucleus (Hong and Carlson, 2007); thereby, Mig1 is not phosphorylated and remains nuclear (Ye *et al.*, 2008). It seems that the Snf1-dependent induction of *ENA1* under salt stress, which is crucial for salt tolerance, is performed through Nrg1 inhibition (Ye *et al.*, 2008). In contrast, after a high pH stress, Mig1, Mig2, and Nrg1 no longer repress *ENA1* expression (see section 2.5) (Platara *et al.*, 2006).

The adaptive responses to glucose scarcity and alkaline pH are closely related. For instance, the alkali-sensitive phenotype of a *snf1* mutant strain is suppressed by adding higher amounts of glucose to the medium, suggesting that an alkaline pH stress mimics a situation of glucose starvation (Casamayor *et al.*, 2012). Snf1 has an important role in the remodeling of gene expression triggered by a high pH stress: it upregulates the expression of 38% of the short-term induced genes under this condition. Around 75% of these genes were also dependent on Snf1 for its induction under low glucose conditions (Casamayor *et al.*, 2012), further reinforcing the idea that an adequate response against glucose scarcity is essential for adaptation to alkaline conditions. Most of these genes are related to carbohydrate metabolism, sugar transport, and glycogen synthesis.

Snf1 also contributes to alkaline pH tolerance by maintaining sufficient levels of acetyl-CoA, the depletion of which results in global histone hypoacetylation (Zhang *et al.*, 2013). Snf1 prevents this depletion by inhibiting transcriptionally and posttranslationally the acetyl-CoA carboxylase Acc1, which transforms acetyl-CoA to malonyl-CoA, and by inducing the expression of the acetyl-CoA synthase-encoding gene *ACS1* via Mig1 and Cat8 (Mitchelhill *et al.*, 1994; Zhang *et al.*, 2013).

2.4. Other pathways involved in alkaline pH adaptation

THE CWI PATHWAY

The *S. cerevisiae* cell wall plays a major role in various aspects of the cell physiology such as protection against osmotic shock, cell shaping, or coping with environmental stresses. When facing a straining situation for the cell wall, the cell wall integrity (CWI) pathway triggers a signaling cascade to respond to the stress and allows the cell to adapt to it.

The plasma membrane proteins Wsc1-3, Mid2, and Mtl1, proposed to function as cell-surface mechanosensors (Dupres *et al.*, 2009; Rajavel *et al.*, 1999), detect cell wall stress and transmit the signal downstream (Ketela *et al.*, 1999; Verna *et al.*, 1997). These sensors are only partially redundant, since Wsc1 is the main activator of the CWI pathway under a heat shock stress (Verna *et al.*, 1997) but Mid2 is the one required for its activation in the presence of the mating pheromone or the cell wall damaging agent calcofluor white (Ketela *et al.*, 1999). Indeed, a mutant strain lacking both *WSC1* and *MID2* can only proliferate in a medium containing sorbitol for osmotic support (Ketela *et al.*, 1999), thus suggesting some complementary functions. The activation of these sensors leads to their interaction with the guanosine nucleotide exchange factors Rom1/Rom2 (Philip and Levin, 2001), which in turn activate the GTPase Rho1 (Ozaki *et al.*, 1996). Among other targets, GTP-Rho1 activates the protein kinase C Pkc1 (Nonaka *et al.*, 1995), starting a MAPK cascade consisting of the MAPKKK Bck1, the apparently redundant MAPKK Mkk1 and Mkk2, and the MAPK Slt2/Mpk1 (Irie *et al.*, 1993; Lee and Levin, 1992; Lee *et al.*, 1993; Torres *et al.*, 1991). An active Slt2 phosphorylates the transcription factors Rlm1 and Swi4/Swi6 inducing the expression of numerous genes related to the cell wall (Madden *et al.*, 1997; Watanabe *et al.*, 1997).

The CWI pathway regulates several cellular processes related to the cell wall. It controls cell wall biogenesis through the β-1,3-glucan synthase enzymes Fks1 and Fks2: GTP-Rho1 stimulates their activity and the transcription factors Swi4/Swi6 induce their transcription (Drgonová *et al.*, 1996; Igual *et al.*, 1996; Qadota *et al.*, 1996). It has also been implicated with cell-surface expansion by associating GTP-Rho1 with the exocytosis component Sec3 (Guo *et al.*, 2001) and is essential for pheromone-induced morphogenesis (Errede *et al.*, 1995). As mentioned, the pathway plays a crucial part in the adaptation to various cell wall stresses such as heat shock, hypo-osmotic stress, or the presence of cell wall damaging agents (Kamada *et al.*, 1995; Ketela *et al.*, 1999).

Under alkaline pH conditions, a proper activation of the CWI pathway is essential for survival, as demonstrated by the alkali-sensitivity of mutant strains lacking *BCK1* or *SLT2* (Serrano *et al.*, 2004). A high pH stress is sensed by Wsc1 prompting Slt2 phosphorylation through the MAPK cascade (Serrano *et al.*, 2006). Activation of Slt2 under this condition upregulates the short-term expression of 18 genes, including the β-1,3-glucan synthase *FKS2* and the cell wall protein-encoding genes *SKT5* and *DFG5*, whose expression is required for alkaline pH tolerance (Serrano *et al.*, 2006).

THE PKA PATHWAY

The protein kinase A (PKA) pathway is involved in the control of metabolism, stress resistance, and proliferation. PKA, an hetero-tetramer composed of two catalytic subunits, encoded by the partially redundant *TPK1*, *TPK2*, or *TPK3,* and two regulatory subunits, encoded by *BCY1* (Toda *et al.*, 1987a, 1987b), is activated by cAMP in response to glucose availability. Intracellular phosphorylated glucose triggers the activation of the GTPases Ras1/Ras2 which in turn stimulate cAMP synthesis by the adenylate cyclase Cyr1 (Beullens *et al.*, 1988; Toda *et al.*, 1985). In addition, extracellular glucose is sensed by the G-protein coupled receptor Gpr1, activating Gpa2 which stimulates Cyr1-mediated cAMP production (Kraakman *et al.*, 1999; Kübler *et al.*, 1997). cAMP binds to the regulatory subunit Bcy1, promoting the hetero-tetramer dissociation and activation of the catalytic subunits (Kuret *et al.*, 1988). This process is negatively regulated by Ira1/Ira2 through Ras1/Ras2 inhibition (Tanaka *et al.*, 1989, 1990).

PKA exerts several functions by regulating gene expression, protein synthesis, and enzyme activities. PKA downregulates the expression of several stress-related genes by phosphorylating the nuclear localization signal of the transcription factor Msn2, which prevents its nuclear import (Görner *et al.*, 1998). Msn2, along with Msn4, induce the expression of the stress responsive element (STRE) controlled genes, related to general stress adaptation and carbohydrate metabolism (Estruch and Carlson, 1993; Martínez-Pastor *et al.*, 1996). PKA also regulates gene expression by inhibiting the kinases Yak1 and Rim15, which activate the transcriptions factors Msn2/Msn4, Hsf1, and Gis1, also involved in the activation of stress response genes (Cameroni *et al.*, 2004; Garrett *et al.*, 1991; Lee *et al.*, 2008a; Reinders *et al.*, 1998). Apart from repressing stress-related genes, PKA stimulates the transcription of ribosomal protein genes and of rRNA/tRNAs through Sfp1 activation and inhibition of Maf1, a transcriptional activator and a RNA polymerase III inhibitor, respectively (Marion *et al.*, 2004; Moir *et al.*, 2006). Independently of transcriptional regulation, PKA modulates the activity of some metabolic enzymes: by inhibiting the glycogen synthase Gsy2 and the trehalose synthase complex, PKA promotes the mobilization of these reserves (Hardy *et al.*, 1994; Panek *et al.*, 1987).

PKA negatively regulates adaptation to alkaline pH: mutations that activate the pathway cause an alkali-sensitive phenotype whereas mutant strains with impaired PKA activity are alkali-tolerant (Casado *et al.*, 2011). Interestingly, mutations increasing Ras2 activity displayed increased sensitivity but mutations increasing Gpa2 activity did not. A high pH stress triggers a transient cAMP decrease, inactivating PKA and thus allowing Msn2 nuclear localization. Ten minutes after an alkaline pH stress, 50% of the induced genes are regulated, at least in part, by Msn2/Msn4, many of them related to glucose, glycogen, and trehalose metabolism (Casado *et al.*, 2011). However, the impact on gene expression of these transcription factors 30 minutes after the stress is much less significant. It is worth mentioning that the Crz1 transcription factor and the Snf1 kinase, both activated during a high pH stress, downregulate Msn2 activity. It has been described that Crz1 provokes Msn2 destabilization in the nucleus and that Snf1 hinders Msn2 nuclear localization (Mayordomo *et al.*, 2002; Takatsume *et al.*, 2010). The opposite regulation by PKA and Crz1/Snf1 of Msn2 under this stress condition may explain its transient effect.

IRON STARVATION RESPONSE

Iron is an essential micronutrient required for several enzymatic reactions. Even though it is quite abundant in the environment, most of it is present as ferric oxyhydroxides, which are poorly soluble at neutral or alkaline pH. On the other hand, it may generate reactive oxygen species that are harmful for the cell. Thus, iron homeostasis must be tightly regulated. In *S. cerevisiae*, the genes implicated in iron homeostasis are regulated by the transcription factors Aft1 and, to a lesser extent, Aft2 (Blaiseau *et al.*, 2001; Yamaguchi-Iwai *et al.*, 1995). Aft1 activity is regulated by intracellular iron levels: an elevated iron concentration triggers nuclear export and inactivation of Aft1 by iron-sulfur clusters and glutaredoxins (Chen *et al.*, 2004; Pujol-Carrion *et al.*, 2006). Under iron starvation conditions, Aft1 is localized into the nucleus where it induces the expression of genes required to increase iron uptake and mobilization of iron from intracellular stores. Many of these genes are plasma membrane iron transporters (*FTR1*), iron oxidases and reductases (*FRE1*, *FRE2*, *FET3*), and siderophore transporters (*ARN1-4*, *FIT2*) (Rutherford *et al.*, 2003).

It has been described that an alkaline pH stress mimics the response to iron starvation probably due to a decrease in iron solubility. The first evidence is the alkali-sensitive phenotype of strains with an impaired response to iron starvation, such as the *aft1* or *fet3* mutant strains (Serrano *et al.*, 2004). More interestingly, only the overexpression of two genes, the low-affinity iron transporter *FET4* and the high-affinity copper transporter *CTR1*, conferred tolerance to alkaline pH conditions. An adequate copper uptake is indispensable for high-affinity iron transport since Fet3 requires copper for its function (Dancis *et al.*, 1994). In fact, the *mac1* mutant strain, lacking the transcription factor needed for *CTR1* expression, is highly sensitive to alkaline pH. Thus, the beneficial effect of an increased copper uptake to cope with high pH stress is probably its impact on iron transport (Serrano *et al.*, 2004). Furthermore, alkaline pH stress induces the expression of several iron, siderophore, and copper transporters, and addition of iron or copper to the medium dramatically improves growth under these conditions (Serrano *et al.*, 2004). All this evidence demonstrates that both metals are important limiting factors to proliferate in alkaline environments. Rim101 also participates in iron homeostasis, since *FET4* expression is partially dependent on this transcription factor during a high pH stress (Lamb and Mitchell, 2003).

RESPONSE TO OXIDATIVE STRESS

A screen for mutant strains sensitive to alkaline pH showed that cells lacking *SOD1* or *SOD2*, encoding superoxide dismutases, grew poorly under this conditions (Serrano *et al.*, 2004), and, in parallel, it was demonstrated that a high pH stress indeed provokes oxidative stress (Viladevall *et al.*, 2004). Moreover, transcriptomic analysis of the response to alkaline conditions revealed the induction of genes related to an oxidative stress response, such as

SOD1, the thioredoxin peroxidase *PRX1*, the glutaredoxin *GRX2*, and the thioredoxin reductase *TRR1* (Serrano *et al.*, 2002; Viladevall *et al.*, 2004). In the case of *PRX1*, it was demonstrated that its alkaline induction depends on the transcription factors Yap1 and, partially, Skn7 (Viladevall *et al.*, 2004). Both factors are responsible for the transcriptional response to oxidative stress and have partially redundant roles (Kuge *et al.*, 1997; Morgan *et al.*, 1997).

Apart from the canonical pathways involved in oxidative stress response, some evidence suggests that other factors may be helping to resist oxidative stress triggered by alkalinization. For instance, the transcription factors Msn2/Msn4, which become transiently active after high pH stress (see above), are responsible for *CTT1* expression, encoding a cytosolic catalase essential for tolerance to oxidative stress (Izawa *et al.*, 1996; Martínez-Pastor *et al.*, 1996). Rim101 plays a protective role against oxidants selenite, *tetr*-Butyl hydroperoxide, and diamide in a Nrg1-dependent fashion (Pérez-Sampietro and Herrero, 2014). In this case, as well as in response to high pH stress, Rim101 requires Rim8, Rim13, and ESCRT proteins to be activated (see section 2.1). This protective role is related to the Rim101 function in vacuolar acidification and may be also relevant to cope with the oxidative stress due to alkaline conditions. In addition, the Snf1 kinase is activated by H_2O_2 and confers tolerance in the presence of oxidants selenite, diethyl maleate, *tetr*-Butyl hydroperoxide, and diamide (Hong and Carlson, 2007; Pérez-Sampietro *et al.*, 2013). Like under alkaline conditions, Snf1, when exposed to selenite, becomes phosphorylated in an Elm1-dependent manner (see section 2.3) and its protective role against this agent is related to glutathione metabolism (Pérez-Sampietro *et al.*, 2013). Maintaining a suitable ratio of reduced/oxidized glutathione could be another mechanism by which Snf1 helps overcome a high pH stress.

2.5. The *ENA1* Na^+-ATPase

Potassium plays an essential role in cell physiology as it is required for negative charge compensation and activation of crucial metabolic processes such as protein translation (Lubin and Ennis, 1964). In contrast, sodium and lithium become toxic at a much lower concentration by substituting potassium and other cations, which leads to inhibition of key metabolic routes such as methionine biosynthesis (Murguia *et al.*, 1995). Thus, even though sodium is much more abundant in the environment, yeast cells keep a high intracellular K^+/Na^+ ratio by favoring potassium uptake and actively extruding sodium. Discriminatory uptake is achieved by the potassium transporters Trk1 and Trk2, which selectively import this ion into the cell (Gaber *et al.*, 1988; Ko *et al.*, 1990). Sodium ions enter the cell also through Trk1 and Trk2, although at a lower affinity compared to potassium, and through nonspecific cation transporters. In addition, Na^+ may enter the cell along with phosphate via the high-affinity phosphate transporter Pho89, the only nutrient transporter that requires sodium described in yeast (see section 4) (Ariño *et al.*, 2010; van der Rest *et al.*, 1995).

More than 20 years ago, Rodriguez-Navarro's group described the sodium pump Ena1 and its involvement in alkaline pH tolerance (Haro *et al.*, 1991). In fact, the authors found that *ENA1* expression was upregulated under alkaline conditions, being the first gene described in *S. cerevisiae* to be induced under such circumstances (Garciadeblas *et al.*, 1993). The Na^+-ATPase Ena1 extrudes sodium and lithium using ATP hydrolysis and is the main sodium efflux mechanism in *S. cerevisiae* (Haro *et al.*, 1991). Depending on the strain, there are one to five almost identical open reading frames encoding Ena proteins, but Ena1 is the most relevant in terms of expression (Garciadeblas *et al.*, 1993; Wieland *et al.*, 1995). A strain lacking all Ena proteins is viable but displays a strong sensitive phenotype to Na^+, Li^+, and alkaline pH (Garciadeblas *et al.*, 1993; Haro *et al.*, 1991). The alkali-sensitive phenotype is probably due to the fact that Nha1, a Na^+-K^+/H^+ antiporter and the other sodium extrusion system of *S. cerevisiae*, cannot function at high pH (Prior *et al.*, 1996); therefore, Ena activity becomes essential in an alkaline environment. Under standard growth conditions *ENA1* expression is negligible but in the presence of high concentrations of Na^+, Li^+, or after a high pH stress it is strongly induced (Garciadeblas *et al.*, 1993; Mendoza *et al.*, 1994), as well as under glucose starvation (Alepuz *et al.*, 1997).

In response to mild saline stress, the osmoresponsive MAP kinase Hog1 becomes active and induces the expression of *ENA1* by inhibiting the repressive function of Sko1 (Brewster *et al.*, 1993; Márquez and Serrano, 1996; Proft *et al.*, 2001). Also, independently of Hog1, PKA phosphorylation of Sko1 enhances its repressor activity (Proft *et al.*, 2001). In addition to Hog1, when cells are subjected to a severe saline stress, *ENA1* is further transcribed due to activation of calcineurin and subsequently Crz1 (see section 2.2) (Mendizabal *et al.*, 1998; Mendoza *et al.*, 1994). In fact, the *ENA1* promoter contains two

CDREs where Crz1 binds, being the downstream one the most relevant (Mendizabal *et al.*, 2001). *ENA1* is also repressed by Mig1 and Mig2 (Proft and Serrano, 1999), both of them controlled by the Snf1 kinase (see section 2.3).

The transcriptional response of *ENA1* to an alkaline stress integrates several of the pathways noted above. Under this conditions, its induction is very fast and transient and it does not depend on Hog1, suggesting that this pathway is not activated by alkaline pH (Serrano *et al.*, 2002). Furthermore, two separate elements of the *ENA1* promoter are responsible for its high pH response. The upstream region, denominated alkaline responsive region 1 (ARR1), contains the relevant CDRE and its induction is fully abolished in the presence of the calcineurin inhibitor FK506 or in a strain lacking either *CNB1* or *CRZ1* (Platara *et al.*, 2006; Serrano *et al.*, 2002). In contrast, the alkaline response of the downstream region ARR2 is calcium-independent. Interestingly, mutation of *rim101* decreases expression from the whole promoter, as well as from the ARR1 and the ARR2 regions (Serrano *et al.*, 2002), suggesting that Rim101 acts on different targets along the promoter. Later on it was found that the Rim101-regulated repressor Nrg1, but not Nrg2, repress the Na^+-ATPase and that it binds directly to the *ENA1* promoter (Platara *et al.*, 2006). Additionally, *ENA1* is equally repressed by Mig1 and Mig2 (Platara *et al.*, 2006). Both of these repressors are downregulated by the Snf1 kinase, which becomes activated under alkaline conditions (Hong and Carlson, 2007), and also induces *ENA1* by negatively regulating Nrg1. In summary, the transcriptional response of *ENA1* to an alkaline stress is mediated by three different pathways: the calcineurin pathway, through the transcription factor Crz1, the Rim101 pathway, repressing the Nrg1 repressor, and the Snf1 pathway, downregulating the Mig1, Mig2, and Nrg1 transcriptional repressors. Notably, even though the promoter of *ENA1* contains a STRE (recognized by Msn2/Msn4), its induction after high pH or salt stress is unaffected by the absence of these transcription factors, indicating that this element is not functional (Alepuz *et al.*, 1997).

2.6. Alkaline pH adaptation in other fungi

Fungi dwell in nearly every environment on earth, where they must adapt to a wide variety of situations. This implies a high degree of diversity among this kingdom and therefore the development of a wide range of different strategies to cope with shifting environmental conditions. However, whether growing in soil or at a host's dermis, changes in the external pH are unavoidable and so an adaptive response to these variations is indispensable.

One common feature of the alkaline adaptation in fungi is the Rim101 pathway (called PacC in filamentous fungi). This pathway is present in deuteromycetes, ascomycetes, and basidiomycetes and is well conserved. It was first described in *A. nidulans*, where it was found to drive transcriptional regulation in response to alkaline conditions (Caddick *et al.*, 1986), and later characterized in other fungi. However, although the Rim101/PacC route is the best-studied pH responsive pathway, studies in other fungi revealed that additional factors are involved in the adaptation to this environmental stress as well.

pH Signaling in Aspergillus Nidulans

The PacC signaling pathway mediates the response to high pH conditions in *A. nidulans* and resembles the Rim101 pathway in *S. cerevisiae* (see section 2.1). The signal transduction starts with the plasma membrane proteins PalH, PalI, and PalF, orthologues to Rim21, Rim9, and Rim8 respectively, forming the putative pH sensing complex (Calcagno-Pizarelli *et al.*, 2007). Exposure to neutral or alkaline pH conditions promotes ubiquitination of PalF in a PalH-dependent manner, which leads to its interaction with PalC and the ESCRT protein Vps23 (Hervás-Aguilar *et al.*, 2010). Although not completely demonstrated, the *S. cerevisiae* orthologue of PalC is thought to be Ygr122w (also called Rim23) and both of them contain a Bro1-domain (Galindo *et al.*, 2007; Rothfels *et al.*, 2005). The PalF-PalC-Vps23 interaction triggers the recruitment of additional ESCRT complex proteins to the plasma membrane, along with PalA and PalB, orthologues of Rim20 and Rim13 respectively (Galindo *et al.*, 2007; Rodríguez-Galán *et al.*, 2009). This enables the C-terminal proteolytic cleavage of PacC by PalB, leaving a 53-kDa version (PacC^{53}) equivalent to the truncated and active Rim101 form of *S. cerevisiae*. Interestingly, PacC^{53} is the substrate of a second, PalB-independent proteolytic event yielding the 27-kDa final product PacC^{27} (Díez *et al.*, 2002; Peñas *et al.*, 2007). Only this smaller form of PacC is localized into the nucleus and can regulate transcription during alkaline stress (Mingot *et al.*, 2001; Orejas *et al.*, 1995).

Unlike Rim101, PacC^{27} can act as both a direct repressor and activator of gene transcription (Tilburn *et al.*, 1995). Its role is to repress the expression of those genes whose encoding proteins may be useless or detrimental under alkaline circumstances, such as the secreted acid phosphatase, and to induce those genes whose products are needed for adaptation to high pH, as the alkaline phosphatase (Caddick *et al.*, 1986). This dual function was observed on the promoters of the isopenicillin-N-synthase-encoding gene *ipnA* and the GABA permease-encoding gene *gabA*. Binding of PacC^{27} to the *ipnA* promoter region induces its expression (Espeso and Peñalva, 1996). On the other hand, on the *gbaA* promoter, PacC^{27} competes with the transcriptional activator ItnA, causing a downregulation of the GABA permease (Espeso and Arst, 2000). Unlike *S. cerevisiae*, no other pathways have been directly implicated in this organism in the response to an alkaline stress.

pH Signaling in *Candida albicans*

C. albicans is the most common fungal pathogen in humans. It normally infects mucosal surfaces but in some circumstances it can enter the bloodstream and cause life-threatening diseases (Davis, 2003). This ascomycete can switch between two morphologies depending on the host niche: an acidic environment, such as the vaginal tract, favors the yeast form whereas a neutral/alkaline one, such as the bloodstream, induces hyphal growth (Davis, 2003). Therefore, adaptation to an alkaline environment is crucial for *C. albicans* virulence (Lo *et al.*, 1997).

In comparison with *S. cerevisiae*, *C. albicans* *Ca*Rim101 pathway follows nearly identical steps to activate this transcription factor (Davis, 2003). However, there are some significant differences. Instead of being ubiquitinated, *Ca*Rim8 becomes hyperphosphorylated and this posttranslational modification requires the same machinery that *Ca*Rim101 processing does (Gomez-Raja and Davis, 2012). *Ca*Rim8 is also the target of the *Ca*Rim101 pathway negative feedback loop: *CaRIM8* expression is repressed by *Ca*Rim101 and *Ca*Rim8 is directed to the vacuole for degradation after *Ca*Rim101 activation, leading to a downregulation of the pathway (Gomez-Raja and Davis, 2012). Interestingly, under acidic conditions, *Ca*Rim101 suffers a *Ca*Rim13-dependent proteolytic cleavage that yields a shorter version than that obtained after an alkaline stress. This version does not regulate the transcription of genes associated with the alkaline response but seems implicated in the adaptation to Li^+ and hygromycin B (Li *et al.*, 2004). Additionally, a high pH stress triggers a calcium burst from the extracellular medium resulting in the activation of the calcineurin pathway (Wang *et al.*, 2011).

It is thought that *Ca*Rim101, like PacC, can induce and repress transcription of target genes: its recognition site can be found in promoters of alkali-induced and alkali-repressed genes and a strain lacking *Ca*Rim101 expresses alkali-repressed genes under alkaline conditions (and fails to express the alkali-induced ones) (Davis *et al.*, 2000). *Ca*Rim101 directs alkaline adaptation by regulating morphogenesis, cell wall structure, and iron transport and homeostasis. When exposed to high pH stress, *Ca*Rim101 triggers the switch to the hyphal form required for virulence (Lo *et al.*, 1997; Ramon *et al.*, 1999). Interestingly, *Ca*Nrg1 acts in parallel of *Ca*Rim101 to govern hyphal morphogenesis, not downstream of it (Bensen *et al.*, 2004). Furthermore, *Ca*Rim101 induces the expression of cell wall remodeling genes that contribute to pathogenesis independently of cell morphology (Nobile *et al.*, 2008). It is also responsible for adaptation to the iron deprivation associated with the alkaline environment in the human host since *Ca*Rim101-dependent expression of iron permeases and reductases is essential for growth in iron deprived conditions (Bensen *et al.*, 2004). The calcineurin pathway is also involved in the response to an alkaline stress, as seen by the strong alkali-sensitive phenotype of a strain lacking both *CaRIM101* and *CaCNB1* (Kullas *et al.*, 2007). Of the two *ENA1* orthologues in *C. albicans*, *CaENA2* and *CaENA21*, only *CaENA21* displays a *Ca*Crz1-dependence for its alkaline induction, whereas both of them are regulated by *Ca*Rim101 under alkaline conditions (Kullas *et al.*, 2007). It is worth noting that the *Ca*Crz1 homologue *Ca*Crz2, whose activation is calcineurin-independent, acts in parallel with *Ca*Rim101 for tolerance to high concentrations of lithium (Kullas *et al.*, 2007). The calcineurin pathway was shown to be crucial for pathogenesis in neutral/alkaline host niches, such as the bloodstream, but irrelevant for acidic niches infections, like vaginal candidiasis (Bader *et al.*, 2006).

Apart from its role in the adaptation to high pH stress, the calcineurin pathway is also responsible for tolerance to azoles such as fluconazole (Sanglard *et al.*, 2003). Thus, the presence of calcineurin inhibitors increases the susceptibility to azoles. Similarly, mutant strains with an impaired Rim101 pathway displayed hypersensitivity to azoles (Sahli *et al.*, 2012). In summary, the signaling pathways that respond to an alkaline environment drive the morphological and transcriptional changes required for virulence and, in addition, trigger the mechanisms needed for drug resistance, making them excellent targets for antifungal strategies.

3. Phosphate homeostasis

Inorganic phosphate (P_i) is an essential nutrient for all organisms. It is required for the synthesis of indispensable metabolites such as nucleic acids or phospholipids and for crucial metabolic processes including reversible protein phosphorylation or energy transfer via ATP. Consequently, *S. cerevisiae* has developed a complex array of mechanisms to ensure uptake, sorting and storage of this nutrient.

3.1. Phosphate homeostasis under non-limiting conditions

Phosphate import through the low-affinity (K_m ~ 1 mM) P_i transporters Pho87 and Pho90 is enough to sustain growth in the presence of normal or high concentrations of this nutrient (Bun-ya *et al.*, 1996; Wykoff and O'Shea, 2001). It has been shown that, in the absence of high-affinity phosphate transporters, Pho90 accounts for most of the phosphate uptake (Ghillebert *et al.*, 2011). On the other hand, Pho87, but not Pho90, is capable of P_i signaling (Giots *et al.*, 2003). Pho91, the other low-affinity P_i transporter, is localized in the vacuolar membrane and exports phosphate from the vacuole to the cytosol (Hürlimann *et al.*, 2007). Both Pho87 and Pho90 are able to transport selenite into the cell (Lazard *et al.*, 2010) and they are constitutively expressed regardless of phosphate availability (Auesukaree *et al.*, 2003).

Pho85 is a cyclin-dependent kinase whose general function in environmental and nutrient sensing is to inhibit stress and starvation responses, signaling that the conditions are satisfactory for cell growth and proliferation. It associates with two different subsets of cyclins: the Pho80 subfamily, which directs Pho85 to environmental signaling functions, and the Pcl1/Pcl2 subfamily, related to cell cycle progression (Huang *et al.*, 2007). A role of Pho85 in phosphate homeostasis, as a negative regulator of repressible acid phosphatase synthesis, was soon identified whereas it was subsequently linked to cell cycle regulation by sequence homology (Toh-e *et al.*, 1988; Ueda *et al.*, 1975). Under a non-limiting phosphate concentration, Pho85, in association with the cyclin Pho80, is active and phosphorylates the transcription factor Pho4, which governs the expression of a set of genes that will be required under a situation of phosphate limitation, known as the *PHO* regulon (Kaffman *et al.*, 1994; Ogawa and Oshima, 1990). This phosphorylation occurs at multiple sites and controls Pho4 localization: it blocks its interaction with the importin Pse1, hindering its nuclear import, and promotes interaction with the exportin Msn5, stimulating its nuclear export (Figure 5)(Kaffman *et al.*, 1998a, 1998b; Komeili and O'Shea, 1999). This regulation serves to keep Pho4 in the cytoplasm, excluding it from the nucleus, thus impeding it to exert transcriptional induction of the *PHO* regulon (O'Neill *et al.*, 1996). As expected, the absence of the low-affinity transport system upregulates the expression of the *PHO* regulon, mimicking a phosphate starvation situation (see below) (Auesukaree *et al.*, 2003).

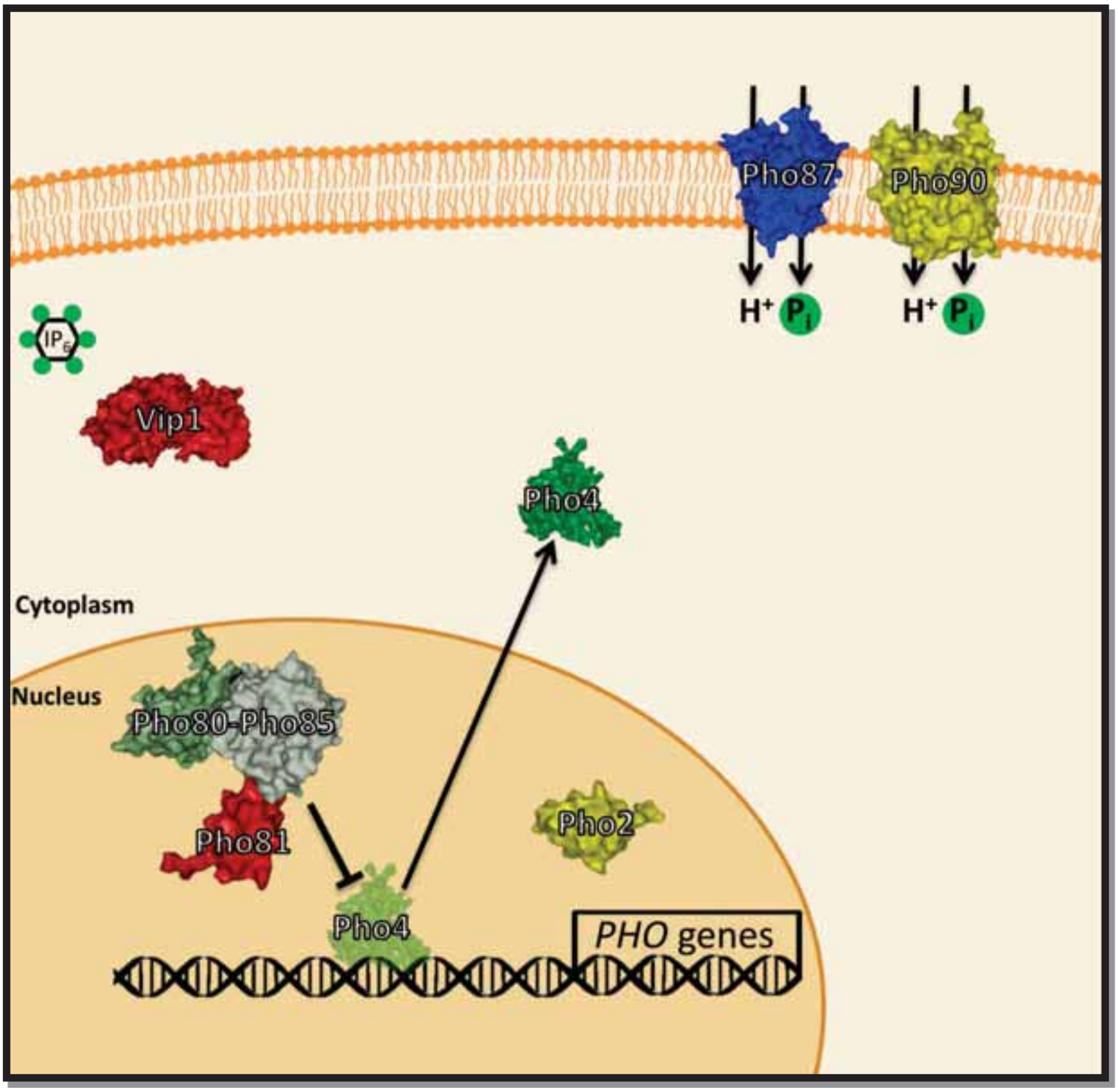

Figure 5. Depiction of the *PHO* pathway under non-limiting phosphate availability. The CDK Pho85, associated with Pho80 and Pho81, phosphorylates Pho4 triggering its nuclear exclusion, thus impeding the transcription of the *PHO* genes. In this situation, the low-affinity phosphate transporters Pho87 and Pho90 cotransport phosphate with protons.

The complex Pho80-Pho85 acts as a link between phosphate availability and cell cycle advance. Under high phosphate conditions, Pho80-Pho85 inhibit by phosphorylation the Rim15 kinase, avoiding entry into stationary phase and promoting cell cycle progression (Wanke *et al.*, 2005). Additionally, Pho85 has been recently found to phosphorylate Cln3, a cyclin involved in progression through G_1 phase (Menoyo *et al.*, 2013). This phosphorylation increases Cln3 stability, favoring entry into S phase. Therefore, when growing with sufficient amounts of phosphate, Pho80-Pho85 hinder cell cycle exit through Rim15 inhibition and stimulates cell cycle progression via Cln3 stabilization (Menoyo *et al.*, 2013).

3.2. Phosphate homeostasis under limiting conditions: the *PHO* regulon

To allow growth and proliferation, yeast cells must ensure an enough cytosolic phosphate concentration to sustain the synthesis of molecules required for cell division, such as nucleic acids or phospholipids. To this end, under conditions of phosphate scarcity, Pho4 directs the upregulation of a diverse set of genes known as the *PHO* regulon. They govern phosphate scavenging, transport, and polyphosphate metabolism in order to maintain the intracellular phosphate pool.

Genes that belong to the *PHO* regulon

Phosphate is mainly imported as free phosphate but it may not be abundant in that form. Instead, this nutrient is often bound to other molecules. *S. cerevisiae* employs extracellular phosphatase activities to scavenge phosphate groups found in macromolecules, making them suitable for the phosphate transporters. *PHO5*, *PHO11,* and *PHO12* are *PHO* regulated genes that encode secreted acid phosphatases (Arima *et al.*, 1983; Bostian *et al.*, 1980; Venter and Horz, 1989). These enzymes suffer multiple glycosylation steps indispensable for their secretion and activity (Schönholzer *et al.*, 1985). It is worth noting that *PHO5* induction under phosphate starvation conditions has been thoroughly studied and its promoter has become a model for transcription factor dynamics and chromatin remodeling (Korber and Barbaric, 2014). In addition, since Pho5 accounts for more than 90% of the total acid phosphatase activity, monitoring this enzymatic activity has been used as a marker for *PHO5* expression and therefore for *PHO* pathway upregulation (Huang and O'Shea, 2005).

The *PHO* regulon also includes an alkaline vacuolar phosphatase encoded by the gene *PHO8* that dephosphorylates phosphopeptides and differs from other protein phosphatases (Donella-Deana *et al.*, 1993; Kaneko *et al.*, 1985).

Under conditions of external phosphate scarcity, the phosphate transporters Pho87 and Pho90 cannot maintain a proper influx of this nutrient due to their low-affinity, resulting in a decrease of the internal phosphate levels. To cope with this situation, the genes encoding the two high-affinity phosphate transporters, *PHO84* and *PHO89*, are expressed in a Pho4-dependent manner (Figure 6)(Bun-Ya *et al.*, 1991; Martinez and Persson, 1998; Ogawa *et al.*, 2000). The proton-coupled high-affinity transport, later found to be mediated by Pho84, cotransports P_i with 2-3 protons, consuming the proton gradient across the plasma membrane in that process, with a K_m of 1-15 µM and an optimum pH for transport at 4.5 (Bun-Ya *et al.*, 1991; Cockburn *et al.*, 1975). Pho84 is responsible for most of the high-affinity phosphate uptake under standard growth conditions (Pattison-Granberg and Persson, 2000) and has been described to mediate arsenate and selenite import (Lazard *et al.*, 2010; Shen *et al.*, 2012). Apart from its strong dependence on the Pho4 transcription factor, *PHO84* is under the transcriptional control of antisense RNAs: in cells grown in sufficient phosphate levels, antisense RNAs recruit histone deacetylases to its promoter thus inhibiting transcription (Camblong *et al.*, 2007, 2009). Pho84 has been described as a transceptor, that is, a transporter with signaling capabilities. Upon P_i readdition to phosphate starved cells, Pho84 rapidly activates the PKA pathway (Giots *et al.*, 2003). This activation depends on P_i uptake and prompts Pho84 own internalization and degradation (Lundh *et al.*, 2009)

Pho89, the other high-affinity phosphate transporter, mediates a Na^+-dependent cotransport of phosphate at a K_m of 0.5 µM with an optimum pH of 9.5 (Martinez and Persson, 1998). Due to its high optimum pH, Pho89 activity is fairly irrelevant for phosphate uptake in standard growth conditions i.e. at acidic conditions (Martinez and Persson, 1998; Pattison-Granberg and Persson, 2000). As a *PHO* regulated gene, *PHO89* is induced by Pho4 in a situation of phosphate scarcity (Ogawa *et al.*, 2000). However, this gene is also strongly upregulated by alkaline pH stress and this induction is in part dependent on the calcineurin pathway (Serrano *et al.*, 2002). For a detailed description of Pho89 and its regulation see section 4.

A mechanism used to cope with fluctuations of the external phosphate concentration is polyphosphate (polyP) synthesis and accumulation. Inorganic polyP is a linear polymer containing tens to hundreds of phosphate residues and is stored mostly in the vacuole (Urech *et al.*, 1978). When grown in the presence of abundant phosphate, *S. cerevisiae* cells tend to accumulate polyP (Martinez *et al.*, 1998). This polymer is synthesized by the vacuolar transmembrane chaperone (VTC) complex, encoded by genes *VTC1*, *VTC2*, *VTC3*, and *VTC4* (Hothorn *et al.*, 2009), also related to V-ATPase stability and other vacuolar functions (Müller *et al.*, 2003). Deletion of *VTC1* or *VTC4* renders the cell unable to generate polyP whereas deletion of *VTC2* or *VTC3* just reduces its accumulation (Ogawa *et al.*, 2000). Polyphosphates are hydrolyzed by the expolyphosphatase Ppx1 and the endopolyphosphatase Ppn1 (Sethuraman *et al.*, 2001; Wurst *et al.*, 1995).

When cells are exposed to phosphate starvation conditions their polyphosphates reserves are rapidly mobilized (Canadell *et al.*, 2015a; Martinez *et al.*, 1998). This polyP degradation occurs prior to the *PHO* pathway response, suggesting that it may act in parallel with it to cope with phosphate scarcity (Pratt *et al.*, 2004). The mobilization of these reserves enables the cell to maintain constant cytosolic P_i levels right after the shift to a phosphate-depleted medium, allowing for cell growth and proliferation under this condition. In fact, it was observed that the polyP pool can sustain two complete cell divisions (Shirahama *et al.*, 1996). Polyphosphate degradation also serves as a buffer for transient fluctuations in extracellular phosphate levels: in a phosphate-depleted medium, induction of *PHO5* is delayed by polyphosphate mobilization (Thomas and O'Shea, 2005). The *VTC* genes, responsible of polyP synthesis, and *PPN1* are induced under phosphate starvation conditions in a Pho4-dependent fashion (Ogawa *et al.*, 2000).

3.3. The *PHO* signaling pathway

Although the mechanism is still unknown, it has been observed that shifting cells from a phosphate rich to a phosphate depleted medium stimulates the synthesis of inositol heptakisphosphate (IP_7) by the inositol hexakisphosphate kinase Vip1 (Figure 6)(Lee *et al.*, 2007). Vip1 and Kcs1 are the two kinases in *S. cerevisiae* able to phosphorylate inositol hexakisphophate (IP_6), generating distinct isomers of IP_7 (Mulugu *et al.*, 2007; Saiardi *et al.*, 1999). Interestingly, the product of Vip1, but not that of Kcs1, inhibits the Pho80-Pho85 kinase activity via Pho81 (Lee *et al.*, 2007). Vip1 IP_7 interacts non-covalently with the CDK inhibitor Pho81, which is constitutively associated with Pho80-Pho85, and stimulates further interactions between these proteins, resulting in the obstruction of the kinase active site (Lee *et al.*, 2008b; Schneider *et al.*, 1994). As mentioned above, Pho85 kinase activity prevents Pho4 nuclear localization; thereby, downregulation of this activity increases the non-phosphorylated form of Pho4 and subsequently its nuclear accumulation (Figure 6).

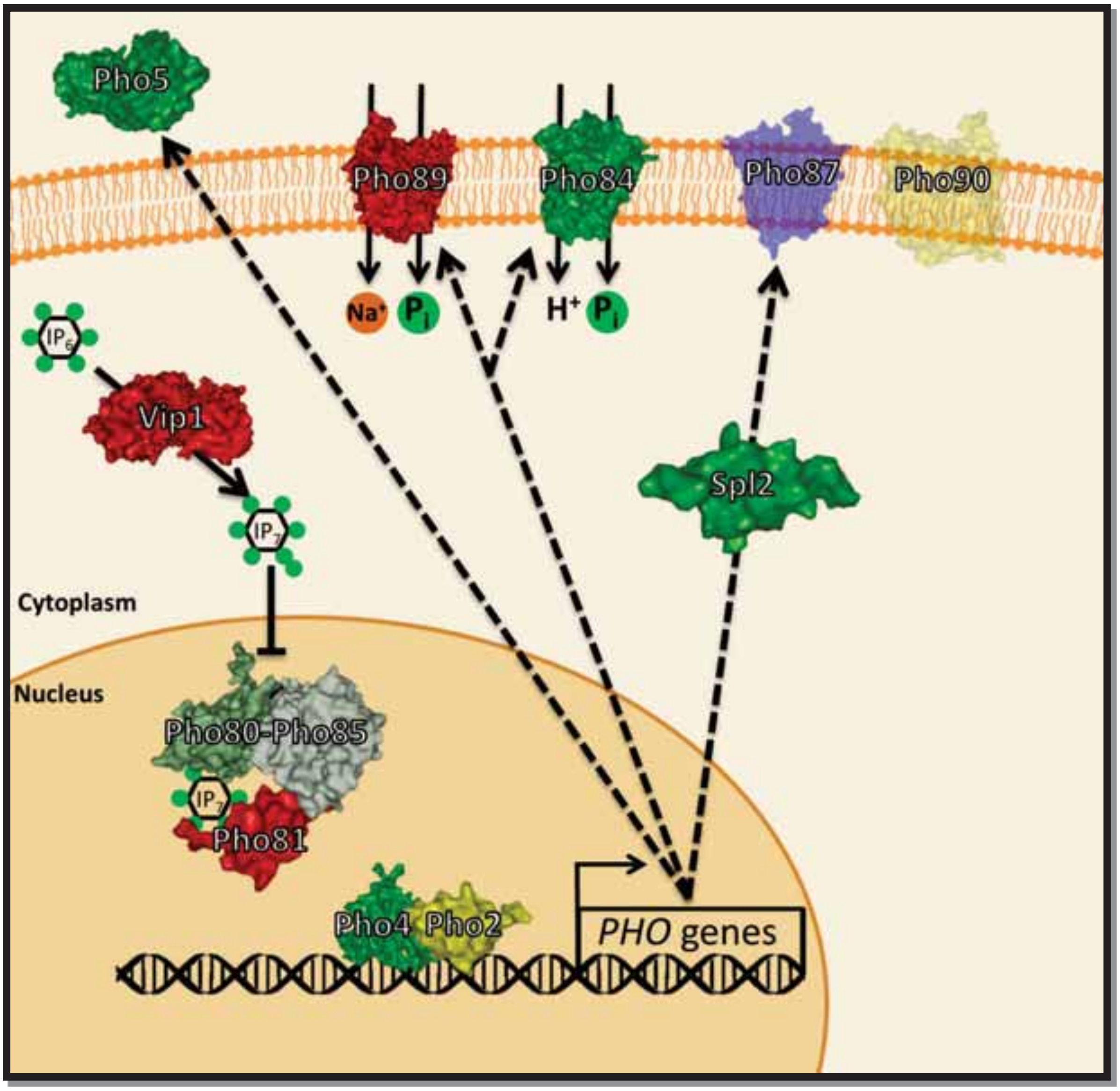

Figure 6. Representation of the *PHO* signaling pathway activation during phosphate starvation. Vip1 phosphorylates IP_6 to form IP_7, which binds to Pho81. This causes the inhibition of Pho85 kinase activity, letting Pho4 to accumulate in the nucleus. In conjunction with Pho2, Pho4 induces the expression of the *PHO* genes, triggering the switch from the low-affinity phosphate transporters Pho87 and Pho90 to the high-affinity transporters Pho84 and Pho89.

Pho4 is a bHLH transcriptional activator that recognizes consensus binding sites found in the promoters of the *PHO* regulon genes (Fisher *et al.*, 1991; Ogawa and Oshima, 1990). It binds the DNA as a homodimer and requires the co-activator Pho2 to induce transcription (Hirst *et al.*, 1994; Shimizu *et al.*, 1997). Pho2 is a homeodomain transcription factor that acts cooperatively with other transcription factors to increase their affinity for the DNA (Brazas and Stillman, 1993). In addition to the *PHO* regulon, Pho2 also regulates the transcription of genes involved in purine and histidine biosynthesis in combination with the transcription factor Bas1 (Daignan-Fornier and Fink, 1992). Pho2-Pho4 cooperativity, which is essential for induction, requires binding of Pho2 to target sites adjacent to Pho4 motifs (Barbaric *et al.*, 1998).

Pho4 binding sites are also recognized by the transcription factor Cbf1. This competitive binding serves two purposes: in high P_i conditions, Cbf1 prevents spurious activation of *PHO* genes by the low level of nuclear Pho4; in low Pi conditions, Cbf1 prevents Pho4 from binding to consensus sites found in non-*PHO* regulon genes (Zhou and O'Shea, 2011). Pho2-Pho4-dependent induction is also regulated by promoter accessibility: it was found that chromatin remodeling complexes, such as the RSC or the SWI/SNF, are necessary for proper transcription of some *PHO* genes (Musladin *et al.*, 2014; Sudarsanam *et al.*, 2000). Notably, the diverse *PHO* genes promoters do not share a common mechanism e.g. the RSC complex intervenes in *PHO5* promoter opening but not in *PHO8* or *PHO84* (Musladin *et al.*, 2014).

Feedback loops governing *PHO* pathway activity

In the last decade it has become evident that the regulation of the *PHO* pathway is considerably complex, including feedback loops and differential regulatory mechanisms for its target genes. As mentioned above, inositol heptakisphosphate (IP_7) is responsible for triggering the activation of the *PHO* pathway, but other inositol polyphosphates also play relevant roles. For example, IP_4 and IP_5, the products of the Arg82 kinase, are required for proper chromatin remodeling leading to full *PHO5* transcription (Steger *et al.*, 2003). In a chemostat culture under low phosphate conditions the expression of *VIP1, KCS1,* and the diphosphorylated inositol polyphosphatase-encoding gene *DDP1* is also induced (Boer *et al.*, 2003). This is somewhat surprising because while higher amounts of Vip1 would activate the *PHO* pathway through the generation of IP_7, the opposite would occur with Kcs1 and Ddp1

(Kcs1 consumes IP$_6$, the same substrate of Vip1, and Ddp1 hydrolyses IP$_7$). It is worth mentioning that additional studies revealed that Pho4 stimulates the synthesis of intragenic and antisense *KCS1* RNAs, promoting the production of truncated Kcs1 (Nishizawa *et al.*, 2008). This would result in an increased IP$_7$ production by Vip1, further activating the *PHO* regulon.

Apart from hindering Kcs1 activity, a complex positive feedback loop keeps stimulating the *PHO* pathway once it has been activated by maintaining decreased internal phosphate levels. As noted above, Pho4 upregulates the transcription of the *VTC* genes, thus promoting polyphosphate synthesis from cytosolic phosphate. Additionally, Pho4 also induces the expression of *SPL2*, encoding a protein responsible for Pho87 degradation (Ogawa *et al.*, 2000; Wykoff *et al.*, 2007). Lower amounts of Pho87 would exacerbate the decrease of phosphate uptake in low phosphate conditions, increasing *PHO* pathway activation. Although Spl2 was described to mediate Pho87 and Pho90 endocytosis, it was later found that Pho90 is degraded in this same condition but in a Spl2- and Pho4-independent manner (Ghillebert *et al.*, 2011). On the other hand, the mechanisms oriented to restore the internal phosphate levels act as a negative feedback loop. The fast induction of *PHO84* reestablish phosphate uptake even in low concentrations of the nutrient, inactivating the *PHO* pathway (Wykoff *et al.*, 2007). Moreover, the polyphosphate mobilization triggered by a decrease in phosphate availability would also downregulate this pathway (Thomas and O'Shea, 2005).

The existence of mutually exclusive states (low- or high-affinity P$_i$ uptake) results in either activation of the *PHO* pathway, relying on the high-affinity P$_i$ uptake, or, instead, inactivation of the pathway, using the low-affinity system to import P$_i$, without an intermediate state. This can be observed in cultures growing at intermediate phosphate concentrations, where some cells exhibit low-affinity P$_i$ transport and the others high-affinity P$_i$ transport (Wykoff *et al.*, 2007). Interestingly, both populations display a similar P$_i$ uptake rate.

SENSING PHOSPHATE AVAILABILITY

To date, the mechanism that regulates the phosphate-dependent synthesis of IP$_7$ by Vip1 is still unknown. However, there is evidence that other inputs contribute to the activation of the *PHO* regulon. Intermediary metabolites of the purine synthesis pathway where shown to influence regulation of the *PHO* pathway. For instance, a mutant strain lacking the adenylate kinase Adk1 shows an increased expression of *PHO84* and this effect is independent of Vip1 but dependent on Pho81 (Gauthier *et al.*, 2008). The authors speculated that the lower ATP-ADP/AMP ratio of this strain might be the cause of this upregulation. Additionally, the *ado1* mutant strain, lacking the adenosine kinase, also shows higher levels of *PHO84* but in a Vip1-dependent manner (Gauthier *et al.*, 2008). Interestingly, the same laboratory described yet another connection between the purine and phosphate pathways. They found that abnormal accumulation of AICAR, a metabolic intermediate of the inosine monophosphate synthesis, stimulates the induction of the *PHO* regulon (Pinson *et al.*, 2009). AICAR promotes the interaction between Pho2 and Pho4, upregulating transcription of the *PHO* regulon genes without requiring Pho4 constitutive nuclear localization (Pinson *et al.*, 2009).

In summary, even though the *PHO* pathway has been thoroughly studied as a model for nutrient-responsive signaling pathways, some fundamental questions remain to be answered. It is accepted that the intracellular phosphate concentration is a signal that controls its activation, but the factor(s) that monitors the levels of this nutrient have not yet been fully identified.

The impact of alkaline pH conditions on phosphate homeostasis

As described above, a pH increase in the external medium results in the activation of adaptive responses associated with the scarcity of some nutrients, such as glucose or iron. Some evidence suggests that phosphate is also a limiting factor during high pH conditions. For instance, an alkaline pH stress causes the induction of several *PHO* regulon genes, including *PHO12*, *PHO84*, *PHO89*, and the *VTC* genes (Lamb *et al.*, 2001; Serrano *et al.*, 2002). Apart from *PHO89*, this induction is fully dependent on Pho4 and follows kinetics similar to that of the transcriptional response to phosphate starvation. Interestingly, the expression of *PHO84* is upregulated already at pH 6.5, which indicates that the *PHO* signaling pathway responds to slight increases in the external pH (Serrano *et al.*, 2002). These transcriptional profiles correlate with the alkali-sensitive phenotype of mutant strains with an impaired *PHO* signaling pathway or missing the high-affinity phosphate transport system, which show a severe growth defect even at neutral pH conditions (Arino, 2010; Serrano *et al.*, 2004).

The activation of the *PHO* pathway in response to high pH stress suggests that an alkaline environment imposes a situation of phosphate starvation to the yeast cell. This is likely caused by a decrease in the phosphate uptake rate when cells are exposed to an alkaline medium. In experiments performed long ago, when the nature of the phosphate transporters was unknown, it was deduced that in *S. cerevisiae* the monovalent form of phosphate was the preferred one to be taken up by the cell (Goodman and Rothstein, 1957; Roomans *et al.*, 1977). This conclusion was inferred from the fact that increasing the external pH, hence decreasing the monovalent phosphate proportion, caused a reduction of the total phosphate uptake. Although this may still be true, there are other important factors to take into account. Alkalinization of the medium implies an activation of the *PHO* pathway and thus switching from the low- to the high-affinity transport system, probably lowering the phosphate uptake rate. In addition, as mentioned in section 2, alkaline conditions perturb the proton gradient across the plasma membrane, compromising the proton-coupled transport of many nutrient transporters. In the case of phosphate transport, this might be especially detrimental because Pho84, Pho87, Pho90, and Pho91 (all except Pho89) use the proton gradient as the driving force to import phosphate. Thus, the destruction of this gradient would deeply impair phosphate uptake for the cell irrespectively of the ionic form of phosphate preferentially taken up.

In conclusion, even though an increase of the external pH does not vary the total amount of phosphate in the medium, this stress deeply disturbs the homeostasis of this nutrient, making the *PHO* signaling pathway indispensable for proliferation at a neutral or alkaline pH.

4. Pho89

4.1. Sodium-phosphate cotransport in *S. cerevisiae*

Sodium-coupled phosphate transport was first characterized by Roomans and coworkers. They found that, at low concentrations of phosphate at pH 7.2, phosphate uptake was enhanced by the addition of Na^+, with a ratio of one phosphate every two sodium ions (Roomans *et al.*, 1977). These authors also described another high-affinity phosphate transport and a low-affinity one, neither of them affected by Na^+. The cation-coupled phosphate transport presented a K_m for Na^+ of 0.6 μM and was also enhanced by lithium. Likewise, the addition of phosphate stimulated Na^+ uptake. Interestingly, the authors discarded the idea that the sodium gradient across the plasma membrane would be the driving force of this cotransport: they measured an intracellular Na^+ concentration of 10 mM but the phosphate uptake was already enhanced by lower amounts of external Na^+ (Roomans *et al.*, 1977). They suggested that the net positive charge of the complex comprised of one monovalent phosphate and two Na^+ ions could be transported along the electrical gradient.

It was not until more than 20 years later, thanks to the sequencing of the *S. cerevisiae* genome, that this transporter was identified as encoded by the ORF *YBR296c* and designated as Pho89 (Martinez and Persson, 1998). Pho89 is the only nutrient transporter that utilizes Na^+ for the coupled transport so far identified in the budding yeast (Ariño *et al.*, 2010; van der Rest *et al.*, 1995). Pho89 is a 574 amino acid protein with 12 predicted transmembrane segments. It has a 45% overall identity sequence with the Na^+/P_i cotransporter Pho-4 of *Neurospora crassa* and 28% with the mammalian type-III Na^+-P_i transporter Pit2 (Martinez and Persson, 1998; Persson *et al.*, 2003). This transporter has an optimum pH for transport at 9.5 and maximal phosphate uptake at 25 mM Na^+, but at 5 mM Na^+ its activity is near maximal already. In contrast, Li^+ and K^+ are much less efficient for phosphate cotransport (Martinez and Persson, 1998). Recently, Pho89 has been successfully expressed in the yeast *Pichia pastori*, allowing for purification and reconstitution of this protein in proteoliposomes (Sengottaiyan *et al.*, 2013). These experiments suggested that Pho89 is found in oligomeric form in detergent solution and, probably, also in the plasma membrane. Additionally, the observation that the Na^+ ionophore monensin impaired the Pho89-mediated uptake of phosphate in proteoliposomes led the authors to conclude that Pho89 utilizes the sodium gradient as a driving force for phosphate transport (Sengottaiyan *et al.*, 2013). This idea contradicts the notion previously reported by Roomans et al., 1977, where they speculated that Pho89 takes advantage of the electrical gradient to facilitate the sodium-phosphate import (see above).

The activation of the *PHO* pathway triggers the downregulation of the low-affinity phosphate transporters (Pho87 and Pho90), leaving the high-affinity ones (Pho84 and Pho89) to take care of phosphate uptake (see section 3.3). Of these, Pho84 accounts for most of the phosphate import in all the conditions tested (i.e. low phosphate at different pHs). This was first deduced when measuring the growth rate of mutant strains lacking Pho84, Pho89 or both proteins. In low phosphate medium, lack of Pho89 doesn't affect the growth rate when compared to the wild type strain, whereas a *pho84* mutant strain shows an impaired growth (Martinez and Persson, 1998). It is worth mentioning that the double mutant strain *pho84 pho89* hardly proliferates, suggesting that, in the absence of Pho84, Pho89 plays a relevant role. Similar results were obtained in alkaline pH conditions: the single mutant strains lacking Pho84 or Pho89 show a wild type phenotype, but the double mutant strain presents a marked alkaline sensitivity (Arino, 2010). These phenotypes are in accordance with the phosphate uptake rates of the strains. The *pho89* mutant strain is still capable to import phosphate even at a pH of 9.5, suggesting that Pho84 is still active under alkaline conditions (Martinez and Persson, 1998). On the other hand, the *pho84* mutant strain shows no phosphate transport at pH 4.5, comparable to the *pho84 pho89* mutant strain, indicating that Pho89 is largely inactive at such a low pH. Thus, under alkaline conditions, phosphate uptake depends on both Pho84 and Pho89. In fact, in experiments performed at pH 8, Zvyagilskaya and coworkers reported that the phosphate transport rate attributable to Pho89 was roughly half of that dependent on Pho84 (Zvyagilskaya *et al.*, 2008).

Pho84 and Pho89 have been shown to transport the phosphate competitor arsenate (Roomans *et al.*, 1977; Shen *et al.*, 2012). Only Pho84 have been described to uptake selenite, although the experimental conditions do not rule out the possibility that Pho89 may also participate in selenite transport (Lazard *et al.*, 2010). In contrast with Pho84, Pho89 cannot act as a phosphate sensor and activate PKA (Zvyagilskaya *et al.*, 2008).

4.2. Regulation of *PHO89*

Basal levels of *PHO89* are barely detectable but, under phosphate starvation conditions, it is induced by Pho4, probably through the Pho4-binding sequences found in its promoter (Martinez and Persson, 1998; Ogawa *et al.*, 2000). Nonetheless, this upregulation was found to be very weak in a wild type strain growing at standard acidic conditions, but increased greatly in the absence of the other phosphate transporters (Auesukaree *et al.*, 2003; Zvyagilskaya *et al.*, 2008). This suggests that in the wild type strain Pho89 has a minor role in the total phosphate uptake but it can take over this function when it is the only transporter available.

Like other members of the *PHO* regulon, *PHO89* is also induced under high pH conditions (Causton *et al.*, 2001; Lamb *et al.*, 2001; Serrano *et al.*, 2002). Surprisingly, it was found that after the alkaline stress, when compared to *PHO84*, *PHO89* expression occurred earlier and lasted for a shorter time (Serrano *et al.*, 2002). The pattern of expression of these genes also differed in their pH dependence: while *PHO84* was already induced at pH 6.5, with a maximal expression around pH 7, *PHO89* started to be significantly expressed at pH 7.5, with a maximal expression at pH 8.2 (Serrano *et al.*, 2002). In addition, the alkaline induction of *PHO89*, but not of the rest of the *PHO* regulon, is under the control of the transcription factor Crz1 (Serrano *et al.*, 2002; Viladevall *et al.*, 2004). Interestingly, the accumulation of *PHO89* mRNA after alkaline stress shows a similar kinetics to that of the Na^+-ATPase *ENA1* which, as mentioned in section 2.5, is also regulated by calcineurin (Serrano *et al.*, 2002). *PHO89* expression is also upregulated when cells are exposed to Congo Red, a cell wall-damaging agent, although this response is independent of Slt2 (Garcia *et al.*, 2004). It is also rapidly induced by Mg^{2+} deprivation in a Crz1-dependent fashion (Wiesenberger *et al.*, 2007). While this work was in progress, a report showed that *PHO89* was induced by the oxidant selenite and, curiously, this response was under the control of Snf1 (Pérez-Sampietro *et al.*, 2013).

OBJECTIVES

In the context of the peculiarity of Pho89's sodium-phosphate cotransport and transcriptional control, not shared by any other *PHO* regulated gene, the aims of this work were:

- To characterize the signaling pathways governing the expression of Pho89 under alkaline conditions and the mechanisms by which this induction takes place.

- To understand the potential biological significance of Pho89 atypical transcriptional pattern and its role in the alkaline pH stress response.

EXPERIMENTAL PROCEDURES

1. Yeast strains and media

S. cerevisiae cells were grown at 28°C in YPD medium (10 g/L yeast extract, 20 g/L peptone, and 20 g/L dextrose). When carrying plasmids, cells were grown in synthetic minimal medium composed of 0.17% yeast nitrogen base (YNB) without ammonium sulfate and amino acids, 0.5% ammonium sulfate, 2% glucose, and 0.13% drop-out mix (lacking the appropriate selection requirements) (Adams *et al.*, 1997). Low phosphate (low P_i) medium was prepared from YNB-based medium without amino acids and phosphate (catalog number CYN0803 [requested to also lack potassium salts]; Formedium Ltd., United Kingdom), which was made 30 mM KCl and 100 µM potassium phosphate (except where otherwise stated). The equivalent high phosphate (high P_i) medium was made by adding 20 mM KCl and 10 mM potassium phosphate. In some experiments, YNB-based medium lacking phosphate and sodium (low NaCl) was employed (catalog number CYN0810; Formedium Ltd.). For preparation of low phosphate agar plates, purified agar (catalog number 1806.05; Conda) was employed. The low-fluorescence minimal medium (lacking riboflavin and folic acid) used for microscopy was prepared as in Verduyn *et al.*, 1992. The yeast strains used in this work are listed in table 1 of Annexes.

2. Recombinant DNA techniques

Escherichia coli DH5α cells were used as a plasmid DNA host and were grown at 37°C in LB (Lysogeny Broth) supplemented, if necessary, with 100 µg/mL ampicillin. Restriction reactions, DNA ligations, and other DNA recombinant techniques were performed as described in Sambrook *et al.* 1989.

DNA fragment purifications, such as PCR products or restriction enzyme digestions, were done by isolating the fragments by agarose gel electrophoresis. The bands of interest were purified using the NucleoSpin Gel and PCR Clean-Up kit (Macherey-Nagel).

E. coli cells were transformed with the standard calcium chloride procedure (Sambrook *et al.* 1989). *S. cerevisiae* cells were transformed following the lithium acetate method as described in Ito *et al.* 1983. For heterologous transformation with disruption cassettes containing the genes *kanMX4* or *nat1*, after the heat shock, cells were resuspended in 0.5 mL of YPD and incubated at 28ºC for 3 hours to allow the expression of the antibiotic resistance to G418 (Calbiochem) or nourseothricin (Werner Bioagents). Afterwards, cells transformed with *kanMX4* or *nat1* cassettes were plated in YPD-G418 (200 µg/mL) and YPD-NAT (200 µg/mL) respectively.

The correct insertion of the recombinant cassettes was verified by colony PCR (Huxley *et al.*, 1990). Yeast cells were deposited at the base of an Eppendorf tube, incubated for 60 sec at the microwave at maximal power, and immediately left at -20°C for 5 min before performing the PCR procedure.

3. Deletion cassettes and gene disruptions

Strains RSC82, ONA1, and ASC13 were constructed by transformation of wild type strain DBY746 with a disruption cassette amplified from the *crz1::kanMX4* (3.0-kbp, oligonucleotides 5'_CRZ1_disr and 3'_CRZ1_disr), *pho84::kanMX4* (2.3-kbp, oligonucleotides PHO84_prom_5' and Clon_PHO84_3'), and *pho89::kanMX4* (2.1-kbp, oligonucleotides PHO89_PROM_5_1 and Pho89_3'_KanMX_2) mutants from the systematic disruption library in the BY4741 background (Winzeler *et al.*, 1999). Strain RSC38 was made by transforming strain ONA1 with a *pho89::TRP1* deletion cassette obtained by amplification of the corresponding locus of strain PAM1 (Pattison-Granberg and Persson, 2000) with oligonucleotides pho89_orf_5' and pho89_orf_3'. Strains ASC17 and ASC30 were constructed by disruption of the *PHO84* and *PHO89* genes with the cassettes described above in the RH16.6 (*ena1-ena4*) background.

Strain RSC22, which carries the *rim101::HIS3* deletion in the DBY746 background, was made by short-flanking replacement with a 1.3-kbp cassette amplified with oligonucleotides 5'disr_RIM101 and 3'disr_RIM101 from plasmid pFA6a-His3MX6 (Longtine *et al.*, 1998).

Strain RSC89 was constructed by transforming the wild type strain DBY746 with a *reg1::kanMX4* cassette obtained by amplification from the BY4741 *reg1* deletion mutant with oligonucleotides 5'-reg1_disr and 3'-reg1_disr. Strain RSC90 was prepared by disruption of *SNF1* with a 3.9-kbp *snf1::LEU2* cassette from BamHI- and HindIII-digested plasmid pCC107 (Rodríguez *et al.*, 2003) in the RSC89 background.

Strain ASC15 was made by deletion of the *PHO4* gene in strain RSC22 (see above) with a deletion cassette (1.6 kbp) obtained from the *pho4::kanMX4* BY4741 deletion mutant. Strain ASC14 was made similarly but by transforming strain RSC10 (Ruiz *et al.*, 2006) with the *pho4::kanMX4* cassette.

Strain MAR193 was made by transforming the *mig2* strain MP010 (Platara *et al.*, 2006) with the *nrg2::kanMX4* cassette described in the same report. Strains MAR197, MAR205, and MAR204 were obtained by transformation of wild type strain DBY746, strain MP018 (*nrg2*), and MAR193 (*mig2 nrg2*), respectively, with the 2.1-kbp *nrg1::nat1* cassette from XbaI- and XhoI-digested plasmid pBS-nrg1::nat1 (Platara *et al.*, 2006).

Strains ASC07, ASC08, ASC09, ASC10, and ASC11, carrying a version of *PHO89* encoding a C-terminally 3 x hemagglutinin (3xHA)-tagged protein, were created by transformation of strains DBY476, MAR15 (*cnb1*), RSC10 (*snf1*), RSC4 (*pho4*), and RSC21 (*rim101*), respectively, with a cassette amplified with primers PHO89-C-pFA6-rev and PHO89-C-pFA6-dir from plasmid pFA6-3HA-His3MX6 (Longtine *et al.*, 1998).

Strain SP011 contains a version of *MIG2* encoding a C-terminally 3xHA-tagged protein integrated into the same chromosomal locus, and was constructed by transforming wild type BY4741 cells with a cassette made by amplification of plasmid pFA6-3HA-kanMX6 (Longtine *et al.*, 1998) using oligonucleotides MIG2-C-pFA6-dir and MIG2-C-pFA6-rev. The same template was employed to amplify cassettes to generate a chromosomally encoded C-terminally 3xHA-tagged version of the *MIG1* or *CRZ1* protein in the BY4741 background (strains SP014 and SP020). The oligonucleotide pairs used were MIG1-C-pFA6-dir/MIG1-C-pFA6-rev (for SP014) and CRZ1-C-pFA6-dir/CRZ1-C-pFA6-rev (for SP020).

Strain ASC28 was constructed by transformation of DBY746 cells with an *ENA1-3xHA-His3MX6* cassette generated by PCR with primers ENA1-C-pFA6-dir and ENA1-c-pFA6-rev and plasmid pFA6-3HA-His3MX6 (Longtine *et al.*, 1998) as the template. Because of the highly conserved sequence of the members of the *ENA* cluster, particular care was taken to ensure the selection of transformants carrying the tag specifically at the C-terminus of the *ENA1* protein. To this end, positive clones were verified with two pairs of primers: ENA1-pFA6-comp-Cter and pFA6a_3HA_rev, which amplify a 0.2-kbp region irrespective of the member of the cluster receiving the tag, and ENA1-pFA6-comp-Nter and pFA6a_3HA_rev, which yield a 3.8-kb amplification fragment specific for *ENA1* integration.

Strains ASC03 and ASC04 were obtained from strains SP014 and SP011, respectively, by transformation with the previously described *snf1::LEU2* cassette (Rodríguez *et al.*, 2003). Strains expressing Mig1-green fluorescent protein (GFP) (SP018) or Mig2-GFP (SP002, SP048, and ASC34) fusions were prepared by transforming either wild type strain BY4741, DBY746, or RSC89 (*reg1*) with amplification fragments obtained by using plasmid pFA6-GFP(S65T)-kanMX6 (for Mig1) or pFA6-GFP(S65T)-HIS3MX6 (for Mig2) (Longtine *et al.*, 1998) and oligonucleotide pairs MIG1-C-pFA6-dir/MIG1-C-pFA6-rev and MIG2-C-pFA6-dir/MIG2-C-pFA6-rev, respectively. The oligonucleotides used in this work are listed in table 2 of Annexes.

4. Plasmids

- **pPHO89-LacZ:** YEp357-based reported plasmid in which the region from positions -671 to +33 (relative to the initiating ATG codon) of *PHO89* is translationally fused to the lacZ gene (Serrano *et al.*, 2002).

- **pPHO89^{CDRE1}-LacZ:** mutation of the upstream CDRE (CDRE1) in pPHO89-LacZ to generate pPHO89^{CDRE1}-LacZ was accomplished by two-step PCR mutagenesis with specific oligonucleotides PHO89_5_CDRE1 and PHO89_3_CDRE1, so the native sequence GTGGCTG was changed to GTG*TA*TG (modified nucleotides are shown in italics).

- **pPHO89^{CDRE2}-LacZ:** mutation of the downstream CDRE (CDRE2) in pPHO89-LacZ to generate pPHO89^{CDRE2}-LacZ was performed by two-step PCR mutagenesis using oligonucleotides pho89_5'_CDRE2_m and pho89_3'_CDRE2_m, which promoted the change from CAGCCAC to CAG*TA*AC.

- **pMM15-PHO84:** allows expression of the Pho84 protein from its native promoter with a 3xHA C-terminal tag. Plasmid pMM15-PHO84 was made by PCR amplification of the relevant *PHO84* locus (nucleotides [nt] -598 to +1760 from the Met initiation codon) with oligonucleotides PHO84_prom_5' and Clon_PHO84_3' (carrying EcoRI- and BamHI-added sites, respectively) and cloning into these same sites of the centromeric plasmid pMM15

(*URA3* marker). Plasmid pMM15 was generous gifts from E. Herrero (Universitat de Lleida, Spain).

- **p**[redacted] containing the entire *ENA1* promoter (from nt -1385 to +35 fused to lacZ), was described previously (Cunningham and Fink, 1996).

- **p**[redacted] drives the expression of the *lacZ* reporter gene from four copies in tandem of the CDREs present in the *FKS2* promoter (Stathopoulos and Cyert, 1997). Used as reporter of calcineurin activation.

5. Growth assays

Sensitivity to alkaline pH in combination with different concentrations of P_i was determined by drop test in low NaCl agar plates buffered with 50 mM TAPS at the appropriate pH, supplemented with 5 mM NaCl and the indicated concentration of KCl and KH_2PO_4. Three µL of the indicated cultures at the optical density at 660 nm (OD_{660}) of 0.05, plus a 10-fold dilution, were deposited on the plate and growth was monitored after 3 days. The same experiment was performed in liquid medium at the indicated pH and concentration of NaCl, P_i, and KCl in 96-well plates. The initial OD_{660} was 0.008 and growth was monitored after 47 hours using the Labsystems iEMS Reader MF (Labsystems).

6. β-galactosidase assays

Yeast cells were grown overnight to saturation in the appropriate drop-out media and then inoculated in YPD at an OD_{660} of 0.2. Growth was resumed until an OD_{660} of 0.5 to 0.7 and cultures were then distributed into 1.0 mL aliquots and centrifuged for 5 minutes at 1620x*g*. The supernatant was discarded and cultures were resuspended in the appropriate media. Alkaline stress was caused by resuspending cells in YPD containing 50 mM TAPS adjusted to pH 8 by addition of potassium hydroxide. Saline stress was provoked by resuspending cells in YPD containing 0.4 or 0.8 M NaCl. Non-induced cells were resuspended in all cases in YPD medium adjusted to pH 5.5. Growth was resumed and cells were collected by centrifugation after 90 minutes of exposure to alkaline pH or 0.8 M NaCl or after 60 minutes of exposure to 0.4 M NaCl. The supernatant was discarded and cell pellets where frozen at -80°C.

In order to perform β-galactosidase assays cells were resuspended in 300 µL of buffer Z (60 mM Na_2HPO_4, 40 mM NaH_2PO_4, 10 mM KCl, 1 mM $MgSO_4$, 35 mM 2-mercaptoethanol). 100 µL of the cell suspension were diluted in 900 µL of buffer Z in assay tubes and cells were permeabilized by addition of 40 µL of chloroform and 20 µL of 0.1 % SDS (sodium dodecyl sulfate) and then vortexed for fifteen seconds. The rest of cell suspensions were stored at 4°C, whereas the assay mixture was placed at 30°C in a water bath. After 15 minutes, 0.2 mL of 4 mg/mL ONPG (o-nitrophenyl-β-D-galactopyranoside) were added to the assay mixture to start the enzymatic reaction (Reynolds *et al.*, 2001). After sufficient yellow color was developed, the enzymatic reaction was stopped by adding 500 µL of 1 M Na_2CO_3. The product formation was evaluated spectrophotometrically at 405 nm in 96-well plates using an iEMS Reader MF apparatus (Labsystems). Concentration of the cell suspensions was monitored similarly, at a wavelength of 650 nm. β-galactosidase activity units were calculated using the formula $[(1000 \times A_{405}) / (\text{time of reaction} \times A_{650})]$.

7. RT-PCR and qRT-PCR

Yeast cells were grown to saturation in YPD overnight and then inoculated in YPD at an OD_{660} of 0.2. Growth was resumed until an OD_{660} of 0.5 to 0.7 and then cells were collected by centrifugation for 2 min at 1620x*g* and resuspended in YPD buffered with 50 mM TAPS at a pH of 8. Cells from 20 mL of culture were collected at the indicated times by rapid vacuum filtration through 0.45-µm Metricel GN-6 filters (Pall Corp.). Cells were quickly frozen in dry ice and stored at -80°C until use.

Total RNA was obtained using the RiboPure-Yeast kit (Ambion) following the conditions indicated by the manufacturer. RNA quality was evaluated by denaturing 0.8% agarose gel electrophoresis and RNA quantification was assessed by measuring A_{260} using Nanodrop 1000 (Thermo Scientific). *PHO89* mRNA levels were determined with 15 ng of total RNA using oligonucleotides RT-PHO89-up1 and RT-PHO89-do1. For determining *ACT1* mRNA levels oligonucleotides RT-ACT1-up2 and RT-ACT1-do2 were used. Semi-quantitative RT-PCR was performed using Illustra Ready-To-Go RT-PCR bead kit (GE Healthcare). Reverse transcription was performed at 42°C for 30 min, and subsequent amplification was carried out for 23 cycles (1 min at 50°C and 72°C for annealing and extension conditions, respectively). qRT-PCR was performed with a CFX96 real-time system (Bio-Rad), using the QuantiTect SYBR green RT-PCR kit (Qiagen).

8. Chromatin immunoprecipitation

Yeast cells were grown overnight to saturation in YPD and then inoculated in YPD at an OD_{660} of 0.2. Growth was resumed until an OD_{600} of 0.6 to 0.8 and then the cultures were induced with 1 M KOH until pH 8 (1 mL per 50 mL of culture). For every time point, 40 mL of culture was made 1% formaldehyde and incubated with gentle shaking at room temperature for 5 min. Then, 2 mL of 2.5 M glycine were added (final concentration of 125 mM) and the samples were incubated as before. Samples were centrifuged at 4°C and 1,800x*g* for 3 min, washed twice with 25 mL of ice-cold HBS buffer (50 mM HEPES pH 7.5, 140 mM NaCl), once with 1.5 mL of Lysis Buffer (50 mM HEPES pH 7.5, 140 mM NaCl, 1 mM EDTA, 1% Nonidet NP-40, 0.1% sodium deoxycholate), and transferred in Lysis Buffer to microtubes. Tubes were then centrifuged at 16,000x*g* for 15 sec, the supernatant was discarded and the pellets were frozen with dry ice and stored at -80°C.

Each pellet was resuspended in 300 μL of ice-cold Lysis Buffer containing 1 mM phenylmethanesulfonylfluoride (PMSF) and Complete, EDTA-free protease inhibitors (Roche). After the addition of 300 μL of zirconia-silica 0.5 mm beads (BioSpec), cells were vortexed briefly and lysed using Fast Prep cell breaker (FastPrep 24, MP Biomedicals) at setting 5.5 for 25 sec (four times). The supernatant was recovered by piercing the bottom of each tube and centrifuging them (220x*g*, 2 min, 4°C) in a 5 ml plastic tube. An additional 300 μL of ice-cold Lysis buffer with PMSF and protease inhibitors was added to the microtube containing the zirconia-silica beads and the supernatant was collected as before (on top of the same 5 ml plastic tube). The final 600 μL were transferred to conical 15 mL plastic tubes (Diagenode) and sonicated using a Bioruptor equipment (Diagenode) for 45 cycles (30 sec ON, 60 sec OFF) at high setting and 4°C to obtain fragments of ≤300 bp. Cell debris was removed by centrifugation (1,800x*g*, 5 min, 4°C) and the supernatant was transferred to new microtubes. The tubes were then centrifuged (9,300x*g*, 5 min, 4°C), the supernatant was transferred to new microtubes, and 10 μL of each sample were separated to new tubes and kept at -80°C (whole cell extracts, WCE).

Samples were pre-cleared with 50 µL of ChIP-grade protein-G-sepharose 4 fast flow (GE Healthcare) for 4 h rotating at 4°C. At the same time, ChIP-grade protein-G-sepharose beads (50 µL per sample) were incubated with 1 µL of anti-HA 16B12 antibody (Covance) per 50 µL of beads under the same conditions. An extra 50 µL of ChIP-grade protein-G-sepharose beads were incubated separately without antibody (no-immunoprecipitation control). Samples were centrifuged (220x*g*, 1 min, 4°C) and the supernatant transferred to new tubes. The ChIP-grade protein-G-sepharose beads mixed with the antibody were centrifuged (220x*g*, 1 min, 4°C), washed with PBS buffer (137 mM NaCl, 2.7 mM KCl, 10 mM Na_2HPO_4, 1.8 mM KH_2PO_4) plus 5 µg/mL bovine serine albumin, and resuspended in the same buffer. Every sample was mixed with 50 µL of beads pre-treated with antibody (and an extra sample with the beads without antibody) and incubated overnight rotating at 4°C.

Each sample was transferred to a 96-well filter plate (Millipore) and centrifuged (220x*g*, 1 min, 4°C). Wells were then washed four times with 250 µL of Lysis Buffer, four times with 250 µL of Lysis Buffer plus 500 mM NaCl, four times with 250 µL of Washing Buffer (10 mM Tris-HCl pH 7.5, 250 mM LiCl, 0.5% Nonidet NP-40, 0.5% sodium deoxycholate, 1 mM EDTA) and two times with TE Buffer (50 mM Tris-HCl pH 7.5, 10 mM EDTA). Finally, samples were resuspended in 200 µL of TE Buffer, transferred to new microtubes, and centrifuged (220x*g*, 1 min, 4°C). The supernatant was removed, and the beads were resuspended in 50 µL of Elution Buffer (50 mM Tris-HCl pH 7.5, 10 mM EDTA, 1% SDS) and incubated at 65°C for 10 min. Afterwards, microtubes were centrifuged (220x*g*, 15 sec), 30 µL of the supernatant was transferred to new microtubes, and 30 µL of Elution Buffer was added to the microtubes containing the beads. Those tubes were incubated again at 65°C for 10 min, centrifuged, and 30 additional µL were transferred to the same microtubes (thus collecting a final volume of 60 µL). 240 µL of Elution Buffer were added to each microtube (including a WCE), sealed with Parafilm, and incubated at 65°C overnight.

Samples were centrifuged (220x*g*, 1 min) and put on ice for 5 min. For each tube, 279 µL of TE Buffer, 6 µL of 10 mg/mL glycogen, and 15 µL of 10 mg/mL Proteinase K were added. Microtubes were then vortexed and incubated at 37°C for 2 h. DNA purification was performed as follows: samples were mixed with 600 µL of phenol:chloroform:isoamylalcohol 25:24:1 (Sigma), vortexed, and centrifuged at 16,000x*g* for 30 min at room temperature. The supernatant was transferred to new microtubes, mixed with 600 µL of chloroform:isoamylalcohol 24:1, and centrifuged again. The supernatant was transferred to new microtubes, mixed well with 4 µL of 5 M NaCl and 1 volume of isopropanol, and kept at -20°C for 1h. Samples were then centrifuged at 16,000x*g* for 10 min at 4°C and the supernatant was discarded. Pellets were dried at 37°C and incubated with 30 µL TE Buffer + 100 µg/mL of RNAse A at 37°C for 5 min. The DNA content of the samples was quantified using Nanodrop 1000 (Thermo Scientific).

For PCR assays, 40 ng of immunoprecipitated DNA was used with oligonucleotides 18Right and 23Left for 28 cycles (1 min at 55°C and 72°C for annealing and extension conditions, respectively).

9. Protein immunodetection

9.1. Sample collection

Yeast extracts for protein extraction and immunodetection were prepared as follows. For low phosphate stress, 50 mL of cells were grown until OD_{660} reached 0.6 in high P_i medium, and cells were collected by centrifugation (3 min at 1,228x*g*), rinsed with low P_i medium, and resuspended in 50 mL of low P_i medium. For alkaline stress experiments, 50 mL of cultures grown on YPD or YNB-based (low or high P_i) medium (pH 5.8) up to an OD_{660} = 0.6 were shifted to pH 8.0 by the addition of the appropriate volume of a 1 M KOH stock solution (1 mL per 50 mL of culture). For salt stress, the appropriate amount of solid NaCl was added to the cultures grown in YPD. For Pho89, Pho84, and Ena1 detection, 5 mL of cells were collected at the indicated times by rapid vacuum filtration through 0.45-µm Metricel GN-6 filters (Pall Corp.). Cells were quickly frozen in dry ice and stored at -80°C until use. To detect phosphorylated Snf1 and the Snf1 protein, as well as the mobility shift of Mig1 and Mig2 upon alkaline pH and salt stress, trichloroacetic acid (100%) was added to the cultures (5 to 10 mL) to reach a final concentration of 5.5%. Cultures were stored on ice for 15 min, and the pellet was collected by centrifugation (2 min, 4°C, 1,200x*g*), transferred to microtubes, washed twice with 1 mL of acetone, air dried at 37°C, and stored at -80°C.

9.2. Extracts preparation

Protein extracts for Pho89, Pho84, and Ena1 determination were prepared as previously described in Horak and Wolf 2001. Cell pellets were resuspended in 1 mL of Milli-Q water with 7.5% 2-mercaptoethanol plus 150 µL of 1.85 M NaOH and were incubated for 10 min at room temperature. Afterwards 150 µL of 50% trichloroacetic acid were added and the samples were incubated for 10 min on ice. Pellets were collected by centrifugation at 13,000x*g* for 10 min, washed with 500 µL of Tris 1 M and resuspended in 120 µL of 50 mM Tris-HCl pH 6.8 containing 8 M urea, 5% SDS, 0.1 mM EDTA, and 1.5 mM dithiothretiol. After incubation at 37°C for 15 min samples were centrifuged at 13,000x*g* for 20 min and the supernatant was transferred to new tubes. Protein quantification was performed using the RCDC Protein Assay (BioRad).

For Mig1 and Mig2 monitoring, protein extracts were prepared as previously described in González *et al.*, 2013 and Urban *et al.*, 2007. Cell pellets were resuspended with 100 µL of urea buffer without EDTA (50 mM Tris pH 7.5, 6 M urea, 1% SDS) and cell lysis was performed with zirconia-silica 0.5 mm beads (BioSpec) by vigorous shaking in a Fast Prep cell breaker (FastPrep 24, MP Biomedicals) at setting 5.0 for 45 sec (5 repeats). Samples were incubated at 65°C for 10 min, centrifuged at 15,800x*g* for 10 min and the supernatant was transferred to new microtubes. Protein quantification was performed by the Bradford method (Sigma Chemical Co.). Before electrophoresis, samples were treated with 10 units of calf alkaline phosphatase (Roche) for 90 min at 37°C, in the absence or presence of 50 mM EDTA.

Snf1 was determined in protein extracts prepared as previously described in Orlova *et al.* 2008. Cell pellets were resuspended in 150 µL of TE buffer (10 mM Tris-HCl pH 7.5, 1 mM EDTA), mixed with 150 µL of 0.2 M NaOH and incubated for 5 min at room temperature. The samples were then centrifuged at 10,000x*g* for 1 min and the supernatant was removed. The pellets were gently resuspended in SDS-polyacrylamide gel electrophoresis (SDS-PAGE) sample buffer (80 mM Tris-HCl pH 6.8, 10 mM EDTA, 4% SDS, 20% glycerol, 0.2% bromophenol blue, 5% 2-mercaptoethanol) with a volume of 30 µL per every 1 OD_{660} of cell culture collected. Afterwards the samples were heated at 95°C for 5 min and centrifuged at 10,000x*g* for 5 min.

9.3. SDS-PAGE and immunobloting

Protein extracts were mixed with 4xSDS-PAGE loading buffer (200 mM Tris-HCl pH 6.8, 40% glycerol, 8% SDS, 0.4 % bromophenol blue, to yield a final concentration of 1x), heated for 5 min at 37°C (except for Snf1 immunoblot, see section 9.2) , and resolved by SDS-PAGE at a concentration of 10% acrylamide (except for Ena1, where 7% acrylamide was used). Afterwards, proteins were transferred onto polyvinylidene difluoride (PVDF) membranes (Immobilon-P, Millipore). Membranes were then blocked with TBS-Tween 20 (0.1% Tween-20, 150 mM NaCl, 20 mM Tris-HCl pH 7.6) plus 5% of fat-free powdered milk for 1 h with gentle agitation. In the case of Snf1 detection, membranes were blocked with TBS-Tween 20 plus 5% bovine serine albumin. Incubation with the primary antibody was performed overnight at 4°C with gentle agitation. Membranes were then washed thrice with TBS-Tween 20 for 10 min and incubated with the secondary antibody for 1 h at room temperature and gentle agitation. Finally, membranes were washed thrice with TBS-Tween for 10 minutes.

HA-tagged Pho89, Ena1, and Mig2 were detected by means of mouse monoclonal anti-HA antibody 12CA4 (Roche) at a 1:1,000 dilution in TBS-Tween 20 plus 5% fat-free powdered milk, whereas the HA.11 clone 16B12 monoclonal antibody (Covance) was employed for detection of HA-tagged Pho84 and Mig1. A 1:20,000 dilution in TBS-Tween 20 plus 5% fat-free powdered milk of secondary anti-mouse IgG–horseradish peroxidase (GE Healthcare) was used. Phosphorylated Snf1 and Snf1 protein were monitored with anti-phospho-Thr172-AMPK (#2531, Cell Signaling Technology) and anti-His (#27-4710-01, GE Healthcare) antibodies, respectively, diluted at a 1:1,000 in TBS-Tween 20.

Membranes were stripped by incubation at 50°C for 30 min with striping solution (62.5 mM Tris-HCl pH 6.7, 2% SDS, 100 mM 2-mercaptoethanol). Actin was detected with the (I-19)-R rabbit polyclonal antibody (catalog number sc-1616-R; Santa Cruz Biotechnology) followed by ECL anti-rabbit IgG–horseradish peroxidase secondary antibodies (GE Healthcare). Immunoreactive proteins were visualized with the ECL Select or Prime (for Pho84-HA detection) kits (GE Healthcare). Relative Pho89 and Ena1 protein levels were calculated by the integration of immunoblot signals using GelAnalyzer software after background subtraction.

10. Determination of intracellular sodium accumulation

Cells were grown on low NaCl medium containing 30 mM HEPES (pH 5.5) in the presence of 5 mM NaCl, 10 mM KCl, and 10 mM P_i until the OD_{660} reached 0.3. Cultures were centrifuged at 1,200x*g* for 5 min, washed with the same medium in which the concentration of P_i was reduced to 0.2 mM, and resuspended in this low P_i medium containing 15 mM KCl. Cells were grown for 60 min to induce the high-affinity phosphate transport system and then centrifuged and resuspended in the same medium, which was adjusted to pH 7.8 with 0.9 mL of 1M KOH per 50 mL of culture (which increases the concentration of K^+ to 18.2 mM). Five-milliliter aliquots were taken immediately after resuspension (t0), and subsequent samples were taken at the desired times.

Samples were rapidly filtered through 25-mm-diameter, 0.45-µm Metricel GN-6 filters (Pall Corp.) previously washed with 2.5 mL of a cold 20 mM $MgCl_2$ solution, and cells were washed once with 10 mL of the $MgCl_2$ solution. Cells were recovered with 2 mL of this solution, filtered through a fresh filter, and subjected to a final wash with 10 mL of the $MgCl_2$ solution. Filters were immersed in 10 mL of a 10 mM $MgCl_2$, 0.2 M HCl solution and gently shaken to resuspend the cells. The intracellular sodium concentration was determined in collaboration with Dr. José Ramos (Universidad de Córdoba) by atomic absorption spectrometry as described previously (Rodriguez-Navarro and Ramos, 1984). Membranes used to filter medium without cells were processed in the same way and used for blank values. The number of cells in each aliquot was determined by measuring the OD_{660} at the moment of sampling, assuming that 1 OD unit equals $8x10^6$ cells. A cellular volume of 49 pL was used for calculations, according to data described previously (Navarrete *et al.*, 2010) and our own determinations for strain BY4741.

11. Microscopy

Log-phase yeast cultures expressing GFP fusions growing in a low-fluorescence minimal medium lacking riboflavin and folic acid (Verduyn *et al.*, 1992) were stained with 1 µg/mL of 4',6'-diamidino-2-phenylindole (DAPI) to visualize nuclei. Cell suspensions were placed onto glass-bottom dishes and allowed to settle for a couple of minutes. Alkaline stress was initiated by gentle removal of the medium using a pipette, placing the tip on the corner of the well, and the medium was then quickly replaced by low-fluorescence medium adjusted with 1 M KOH to pH 8.0. Images of living cells were taken before and after initiation of stress at different times with a confocal laser scanning microscope (Leica TCS SP2), using a 63x oil immersion objective.